Rochester Institute of Technology
RIT Digital Institutional Repository

Theses

2010

Exploration of non-chemically amplified resists based on chain-scission mechanism for 193 nm lithography

Meng Zhao

Follow this and additional works at: https://repository.rit.edu/theses

Recommended Citation
Zhao, Meng, "Exploration of non-chemically amplified resists based on chain-scission mechanism for 193 nm lithography" (2010). Thesis. Rochester Institute of Technology. Accessed from

This Thesis is brought to you for free and open access by the RIT Libraries. For more information, please contact repository@rit.edu.

Exploration of Non-Chemically Amplified Resists Based on Chain-scission Mechanism for 193 nm Lithography

By
Meng Zhao

A Thesis Submitted
in Partial Fulfillment
of the Requirements for the Degree of
Master of Science
in
Microelectronic Engineering
Approved by:

Prof. ______________________________
Dr. Bruce W. Smith (Thesis Advisor)

Prof. ______________________________
Dr. Thomas W. Smith (Committee Member)

Prof. ______________________________
Prof. Dale Ewbank (Committee Member)

MICROELECTRONIC ENGINEERING PROGRAM
COLLEGE OF ENGINEERING
ROCHESTER INSTITUTE OF TECHNOLOGY
ROCHESTER, NEW YORK
MAY, 2010

Abstract

In order to achieve the requirement for sub-32nm technology, a substitution to chemical amplified photoresist should be explored because it suffers several problems including acid diffusion, environmental sensitivity, process complexity and critical dimension (CD) control. On the other hand, Poly (Methyl methacrylate) (PMMA) has been used for a long time as a chain-scission resist in E-beam as well as DUV. This kind of photoresist has good resolution and small LER compared to CAR. But it has poor sensitivity and etch-resistance. The main goal of this project is to explore roles of resist components and limitation of resolution, sensitivity and LER.

Photoresist derived from PMMA will have base solubility, adequate sensitivity as well as resolution by incorporating TBMA MAA and αMEST in the polymer backbone. In this project, new polymers will be synthesized and lithographic characterization will be measured including sensitivity, contrast and etch resistance.

Table of Contents

Chapter 1 1

Introduction 1

1.1 Moore's Law and ITRS 2

1.2 Review of Nanolithography Technology 4

1.2.1 Optical Lithography 4

1.2.2 Immersion Lithography 5

1.2.3 EUV Lithography 6

Chapter 2 7

Theory 7

2.1 Photoresist Material 8

2.1.1 i-line Resist System: DNQ-Novolak 8

2.1.2 DUV Resist: PHOST 11

2.1.3 193nm Resist: Acrylic Terpolymer 12

2.1.4 e-beam Resist: Main-chain Scissioning Resist 14

2.2 Limitations of Chemical Amplified Photoresist 16

2.3 Line Edge Roughness 20

2.4 Optical Materials for 193nm Optics 23

2.5 Conclusion 25

Chapter 3 27

Design of Non-Chemically-amplified Resist 27
3.1 Main-chain Scissioning Resist 27
3.2 Main-chain scissioning Resist for 193nm Lithography 30
3.2.1 Base Solubility 30
3.2.2 Sensitivity 31
3.2.4 Etch Resistance 36
Chapter 4 38
Experimental Approach 38
4.1 Material Synthesis 38
4.1.1 PMMA and P(MMA-co-αMEST): 38
4.1.2 P(MMA-co-MAA): 38
4.1.3 P(MMA-co-TBMA-co-MAA): 39
4.1.4 P(ADMA-co-TBMA-co-MAA): 39
4.1.5 Polymer Isolation: 39
4.1.6 Molecular Weight and Composition 39
4.1.7 Polymer Film Fabrication and Characterization 40
Chapter 5 41
Result and Discussion 41
5.1 Enhancement of Sensitivity 41
5.2 Base Solubility 43

5.3 Etch resistance 45

5.4 Silicon-containing Polymer 47

Chapter 6.. 51

Conclusion 51

Reference 53

Chapter 1

Introduction

The semiconductor market has grown at an average annual rate for approximately 15%. This growth has been maintained by the industry's unique ability to consistently provide higher device performance at lower cost (achieving a 25-30% per-year cost reduction per function) [1]. Microlithography is the key technological driving force for this. Generally the overall rate of progress in microelectronics is determined by the growing rate in microlithography tools, method, and materials. A decrease in minimum image size by a factor of two will lead to a factor of four increase in the number of devices that can be built on a given area of the semiconductor chip as well as significant enhancement in transistor speeds. In its original meaning, the term lithography refers to a process of printing using a nonpolar ink applied to a hydrophilic master plate patterned with a hydrophobic image. In its current modern usage, the term is more generally applied to a number of methods for replicating a predetermined master pattern on a substrate. Most commonly, replication is effected by first coating the substrate with a radiation-sensitive polymer film (a resist) and then exposing the film to actinic radiation in a pattern-wise manner [1]. The physical or chemical properties of the exposed areas of the film are altered such that they can be differentiated in a subsequent image development step. Most commonly, the solubility of the film is modified with the radiation chemistry either increasing the solubility of exposed areas (yielding a positive image of the mask after develop) or decreasing the solubility to yield a negative-tone image of the mask [1].

This technology is widely used in microsystem and nanosystems manufacturing process as well as semiconductor fabrication process. Photolithography has been recognized to be the key technology in IC manufacture for a very long time because it plays an important role to define number of discrete devices per integrated circuit. Optical lithography is the main-stream technology in this area. The fast development in the semiconductor industry have demanded optical lithography with the ability of printing smaller critical dimensions (CD) as well as other specifications indicated by the International Technology Roadmap of Semiconductors (ITRS) [2]. Other main-stream lithography technologies include Optical Nanolithography, Immersion Lithography, EUV Lithography and Double Patterning. "Unconventional" Nanopatterning technology refers to Electron Beam, Ion Beam, Maskless Lithography (ML2), Nano-imprint and Self Assembly Block Polymers, etc.

1.1 Moore's Law and ITRS

Gordon Moore published an article in 1965 [3] indicating that the number of transistors that can be placed on unit area has doubled about every two years, achieving the inspiring total of 50–60 devices per chip by 1965. He also predicted that this trend will last for at least 10 years. This trend he predicted has still remained surprisingly accurate at present. Although the doubling time for devices per chip has varied slightly and probably averages closer to 18 months than one year, the exponential trend has been maintained.

Moore's Law has been used widely in economic expectation of semiconductor industry. Researchers on the other hand usually use industry roadmap as the planning tool.

The International Technology Roadmap for Semiconductors (ITRS) is now one of the most important references for the semiconductor industry. It addresses the technological challenges the industry may meet over the next 15 years, indicating possible solutions. Today, all semiconductor-equipment and chip manufacturers follow white papers from the ITRS, when they implement their roadmaps. The 2008 ITRS roadmap is shown in Figure 1.1:

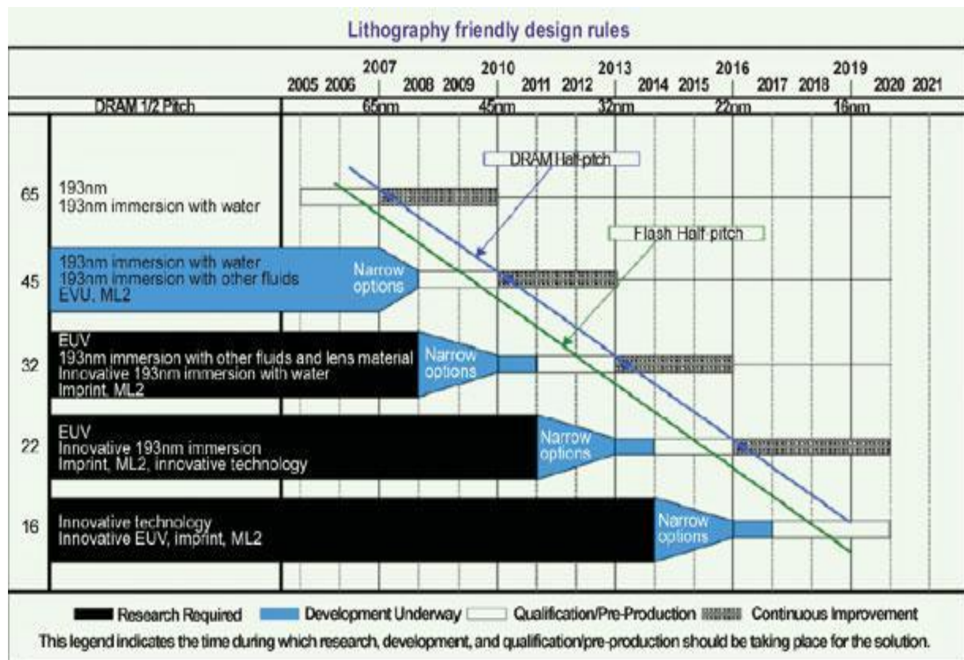

Figure 1.1 2008 ITRS Roadmap [4]

It is noted that optical lithography is encountering stiff challenges when moving to deep submicron production. Conventional optical lithography encounters a bottleneck, as the numerical aperture (NA) approaches 0.9. Changing the wavelength incurs higher costs due to a lack of a mature photoresist and the expense to develop new optical materials. Enhancing resolution via the adoption of off-axis illumination, no matter

whether through the adoption of quadrupole or cross-quadrupole light sources, involves linear issues [4].

There are many new technologies in development, including 157nm, 193nm immersion and extreme ultraviolet (EUV) lithography. All of these technologies have been developing very fast during the past several years. Immersion lithography, based on high-index fluid, enables 193nm lithography to be used in sub-32nm lithography. JSR and Mitsui Chemicals (MCI) have both presented solutions for meeting the challenges of production at 32nm. JSR has developed a high refractive index solution that combines high transparency with low viscosity, to allow a refractive index of 1.64 [4]. This development enables 193nm lithography to be used in sub-32nm lithography.

1.2 Review of Nanolithography Technology

1.2.1 Optical Lithography

Optical lithography uses light to transfer a geometric pattern from a photo mask to photoresist film on the substrate. The first generation of optical lithography is contact lithography. It gives excellent resolution. But since the close contact of mask and wafer, the mask can be contaminated and eventually lose integrity [5]. The contamination and contact-induced damage can be solved by proximity lithography [6], in which a small gap exists between the mask and the wafer. The CD resulting from this method is about 2-3 μm. Projection lithography, on the other hand, is characterized by large gap between mask and wafer. Unlike contact or proximity masks, which cover an entire wafer, projection masks (known as "reticles") show only one die or an array of die (known as a "field"). Projection exposure systems (steppers) project the mask onto the wafer many

times to create the complete pattern. The ability to project a clear image of a small feature onto the wafer is limited by the wavelength of the light that is used, and the ability of the reduction lens system to capture enough diffraction orders from the illuminated mask. Optical lithography is then further classified by wavelength as shown in Table1.1:

Name	wavelength	Projection system
Near UV	350 - 450 nm	i-line 365nm, g-line 436 nm
Mid UV	300 - 350 nm	XeCl 308nm
Deep UV	190 - 300 nm	ArF 193nm, KrF 248nm, Hg
VUV	110 - 190 nm	F2 157nm, others

Table1.1 Optical lithography systems

1.2.2 Immersion Lithography

The minimum feature that can be printed by optical lithography is determined by Equation [1.1], which is also called Rayleigh equation:

$$hp_{min} = \frac{k_1 \lambda}{NA} \quad [1.1]$$

where, k_1 is the resolution factor, λ is the wavelength of the exposing radiation and *NA* is the numerical aperture.

In ArF projection system, it is suggested that NA can be achieved to be as high as 0.93. The resolution limit for 193nm exposure systems may be calculated using the Rayleigh equation with, k_1 = 0.25, NA=0.93 and λ=193nm:

$$hp_{min} = \frac{k_1 \lambda}{NA} = \frac{0.25 \times 193nm}{0.93} = 52nm \quad [1.2]$$

Because the refractive index of air is 1.0, the NA of a projection system with air in between the optical lens and wafers is limited by projection angles. In immersion lithography system, the gap of lithographic lens and wafers must be filled with immersion fluid, which has a refractive index larger than 1.0, extending NA of the projection system. Before this technique was not fully developed because several difficulties such like compatibility to resist, large absorption of immersion fluid in 193nm etc. Besides, there were other options to shrink minimum feature size. Now at NA=1.5, a 32nm half pitch has been demonstrated.

1.2.3 EUV Lithography

Extreme ultraviolet lithography (also known as EUV or EUVL) is a next-generation lithography technology using the 13.5 nm EUV wavelength. It is characterized by a transition in the physics of interaction with matter. Wavelengths longer than about 30 nm interact mainly with the chemical valence electrons of matter, while wavelengths shorter than that interact mainly with inner shell electrons and nuclei. Since all mater absorbs in such short wavelength, EUV lithography need to take place in vacuum. All the optical elements, including the photomask, must make use of defect-free Mo/Si multilayers which act to reflect light by means of interlayer interference; any one of these mirrors will absorb around 30% of the incident light. This limitation can be avoided in maskless interference lithography systems. However, the latter tools are restricted to producing periodic patterns only.

Chapter 2

Theory

Photoresist plays an important role in lithography technology. There are two types of photoresist. A positive resist is a type of photoresist in which the exposed area becomes soluble in developer which unexposed area remains insoluble. A negative resist is a type of photoresist which is soluble initially in developer and upon exposure, becomes insoluble. The development in photoresist system greatly influence the achievable lithographic CD (critical dimension) as well as the quality of patterns transferred to the substrate through the mask.

Specific photoresist system needs to be designed according to the wavelength used in lithography technology. Some properties related to photoresist need to be considered in design. First of all, it should be transparent in the corresponding wavelength to minimize the intensity gradient through the resist film. A photoresist system should have high sensitivity to achieve high throughput in economic point of view. Then a good resist system should have relatively high contrast to ensure pattern quality and high dry-etch resistance for the subsequent process steps. The development trend of lithography system with corresponding photoresist is shown in Figure 2.1

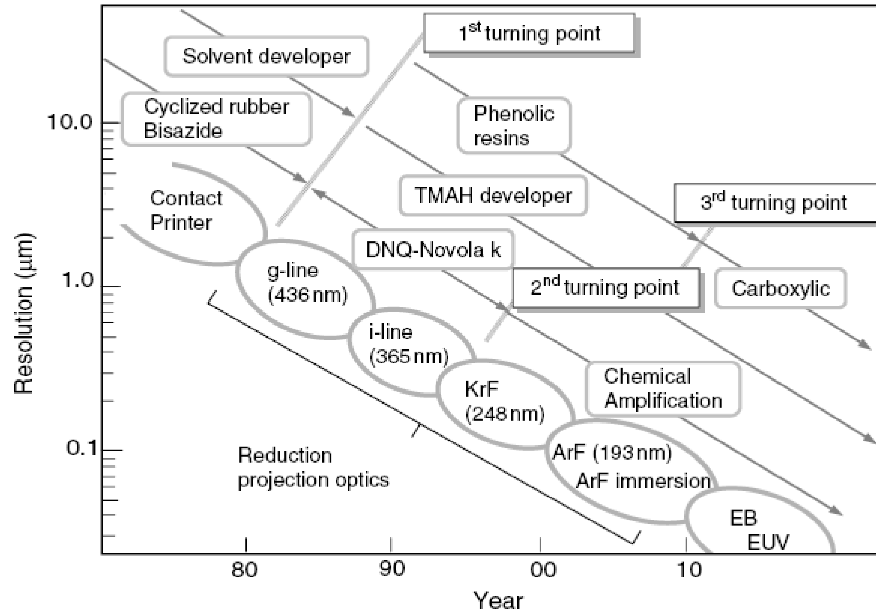

Figure 2.1 Development trend of lithography and resists [1]

2.1 Photoresist Material

2.1.1 i-line Resist System: DNQ-Novolak

This system used to be widely used in early 1980s when i-line was the primary lithography wavelength and sub-300nm was the targeting feature size. It was demonstrated to be a very successful system in terms of contrast and resolution, as well as relatively high sensitivity. Even at present, there are still many researchers putting effort on this system and trying to make further development in this system. These resists contain novolak resin and a diazide napthaquinone (DNQ) photoactive compound. Novolak resin, whose structure is shown in Figure 2.2 (a), is soluble itself in base. Diazonaphthoquinone (DNQ), whose structure is shown in Figure 2.2 (b), is a diazo derivative of naphthoquinone.

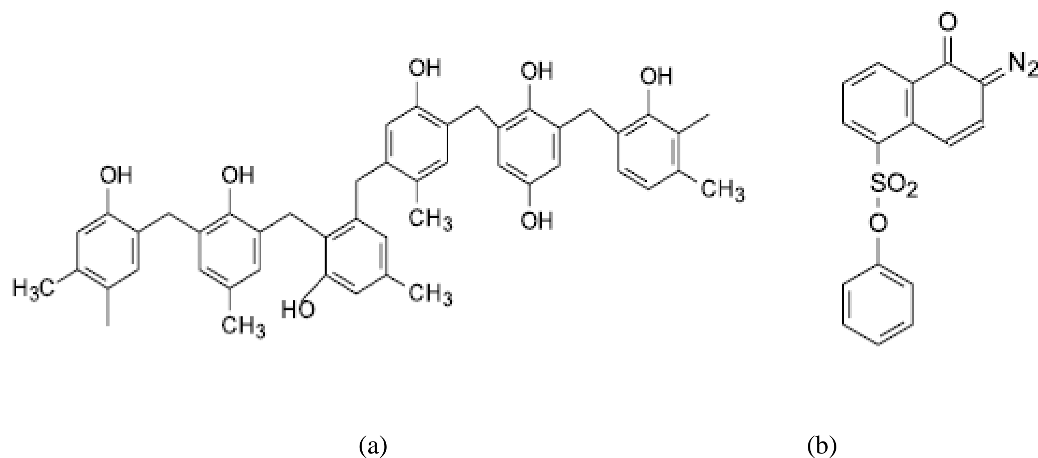

(a) (b)

Figure2.2 (a) Novolak resin which is formed by condensation polymerization (b) DNQ

The central phenomenon of dissolution inhibition resist is the large effect which napthaquiznone derivatives have on the dissolution of novolak film. Novolak itself is soluble in aqueous base. But if it contains a small amount of DNQ, the dissolution rate decreases dramatically. However, if this mixture is exposed to radiation, it dissolves even faster than pure novolak film. It has been proved that the key to dissolution inhibition is the interaction between the sulfonic ester of the PAC and the phenol groups of the novolak resin. When a novolak/DNQ resist film is exposed to radiation, the diazoquinones loose molecular nitrogen and undergo a so-called Wolff rearrangement, leading to ring contraction and eventually to the formation of a carboxylic acid. This process is shown in Figure 2.3:

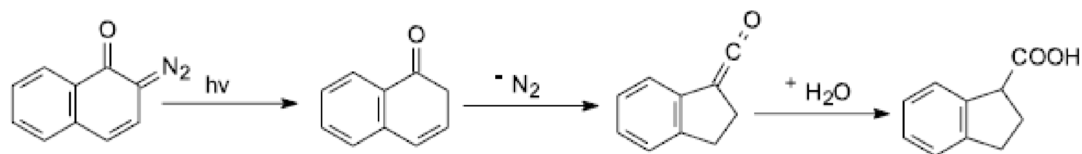

Figure 2.3 Photoreaction of DNQ

A lot of data has been accumulated in order to fully understand the mechanism of this resist system. Impact on resist performance in terms of molecular weight, poly-dispersity and structure of Novolak was investigated thoroughly [7]. A “Stone-wall” model was proposed [7]. It says that in DNQ/Novolak system, DNQ molecule protects small-molecular-weight resin through Azo-coupling reaction [7]. The mixture thus becomes insoluble in base. This Dissolution Inhibition system based on DNQ/Novolak shows high resolution in i-line lithography. However, the absorption of Novolak resin in DUV regime is too high to be used in short-wavelength lithography. The absorption data of both DNA and Novolak is shown in Figure 2.4.

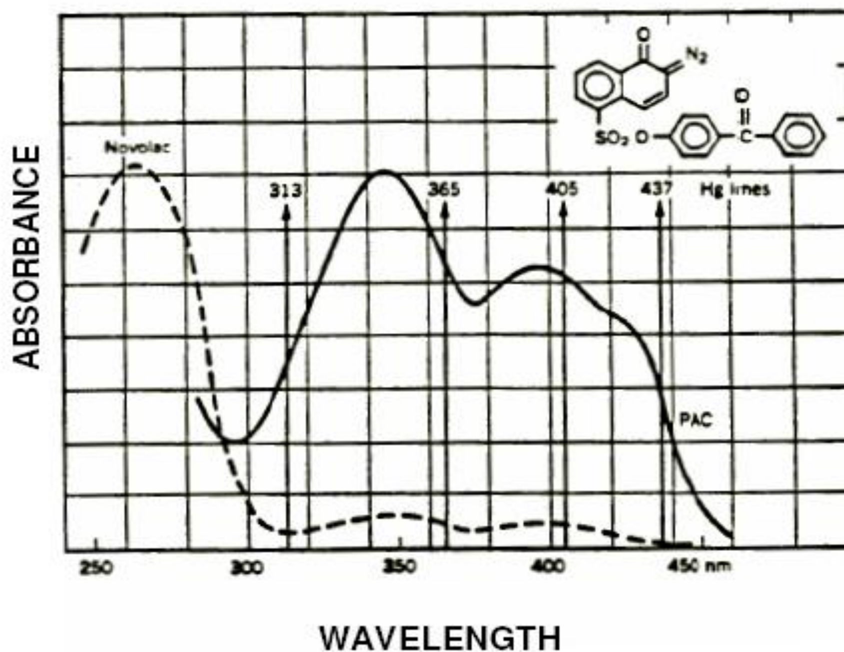

Figure2.4 Absorption data of dissolution inhibition system DNQ/Novolak [1]

2.1.2 DUV Resist: PHOST

Although DNQ/Novolak system has been proved to be an efficient resist platform with high resolution in i-line lithography, the high absorption of Novolak resin prevents its application in DUV lithography. Fortunately, Poly(4-hydroxystyrene) - an isomer of Novolak – is transparent at 248nm. This photoresist based on PHOST utilized totally different mechanism from DNQ/Novolak system. It usually contains photo-acid generator (PAG) which generates acid upon exposure and protected PHOST, so called t-BOC-PHS, which contains acid-labile group, tertiary – Butoxycarbonyl (t-BOC). The photoreaction of PAG and deprotection reaction of t-BOC-PHS is shown in Figure 2.5 (a), (b) respectively [8].

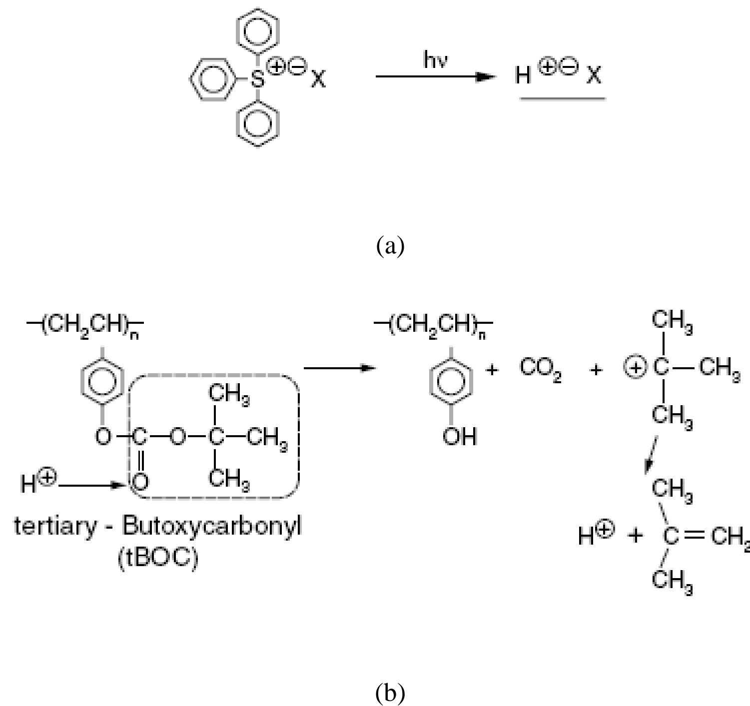

(b)

Figure 2.5 (a) PAG generates acid (b) Deprotection reaction of t-BOC-PHS [8]

The deprotection reaction shown in Figure 2.4 (b) is a process in which the t-BOC group attached on PHS is cleaved by acid generated during exposure, forming base-soluble product. It can be seen that in this reaction, acid is also a product. It can diffuse around during post-exposure bake (PEB) and react with other polymer molecules. Therefore, this is an amplification process in which a single photoevent initiates a cascade of subsequent chemical reactions. This type of resist is so called chemically-amplified photoresist.

2.1.3 193nm Resist: Acrylic Terpolymer

As the requirement of IC device fabrication goes into sub-32nm regime, the ability of 193nm optical lithography faces a challenge, especially in material perspective. Chemically-amplified photoresist is widely used as 193nm resist platform at present because its ability to achieve high through-put. The catalytic action of the photo-generated acid on the photoresist polymer during a post-exposure bake (PEB) step causes a change in the dissolution rate in the exposed areas of the film. A single photo-generated catalyst molecule can facilitate hundreds of chemical reactions that alter the solubility of the exposed regions and thereby provide chemical amplification of the exposure dose. However, CA resist system based t-BOC-PHS can't be used in 193nm because it contains aromatic group which has a high absorption coefficient at this wavelength.

Terpolymer of methylmethacrylate, t-butylmethacrylate, and methacrylic acid was synthesized and demonstrated patterning with 193nm exposure [9]. This terpolymer can be blended with PAG to form a Chemically-amplified resist. Its structure is shown in Figure 2.6 with function of each monomer labeled. Methylmethacrylate provides film qualities such as hydrophilicity and adhesion. It also provides a diffusion barrier which

prevents acid from diffusing out of exposed area. T-Butylmethacrylate provides the protection group (t-butyl group) which can be cleaved by acid to from base soluble product, resulting in a positive image. Methacrylateacid allows base solubility for this polymer so that it can be base developed.

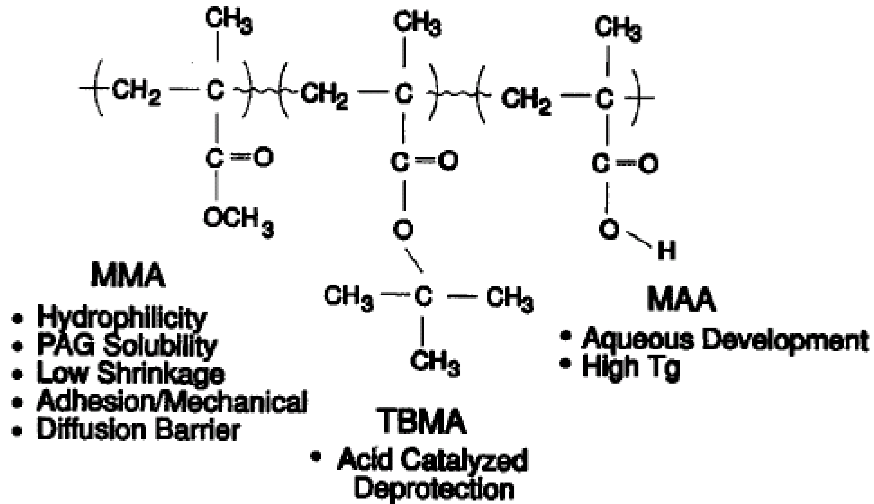

Figure2.6 Template of chemically-amplified photoresist for 193nm [9]

Although shown to have good resolution, this resist system has poor etch resistance. Certain monomers, such like adamantyl methacrylate, can be put in the polymer to provide this property. The structure is shown in Figure 2.7.

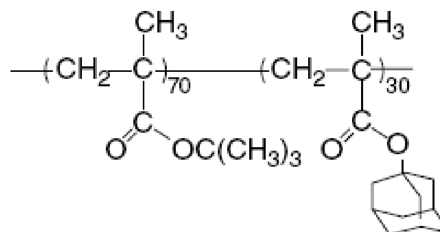

Figure 2.7 Adamantyl-containing CA resist

2.1.4 e-beam Resist: Main-chain Scissioning Resist

A number of polymeric materials which exhibit little or no sensitivity to UV radiation will undergo efficient degradation when exposed to an electron beam. One of the first polymers recognized to exhibit sensitivity to electron-beam radiation was high molecular weight poly-(methyl methacrylate) (PMMA). Electron-solid interactions lead to extensive chain scission of the PMMA chains. The fragmented chains rapidly dissolve in organic developer mixtures to yield positive-tone imaging. Examples of other resist polymers developed specifically for electron-beam lithography and now used commercially include poly(2,2,2-trifluoroethyl-R-chloroacrylate) (sold as EBR-9 by Toray, Inc.), poly(R-chloroacrylate-*co*-R-methylstyrene) (supplied by Nippon Zeon Co as ZEP-520), and poly-(butene-1-sulfone). PMMA is the classical e-beam resist and offers the advantages of extremely high resolution, ease of handling, wide process latitude and ready available. PMMA is easily produced to a high molecular weight by radical polymerization. It has Gs value of 1.3 and has no measurable cross-linking propensity [10]. The radiation induced main-chain scissioning of PMMA has been studied for a long time. The photochemical event appears to be homolysis of carbonyl carbon to main-chain carbon bond followed by rearrangement of main-chain radical through β-scission to cleave the chain and generate an acyl-stabilized, tertiary radical. This process generates fragments of carbon monoxide, carbon dioxide, and methyl and methoxyl radicals. This photoreaction is called "Norrish type-I" process. The mechanism of photo-degradation of PMMA is shown in Figure 2.8 [10]:

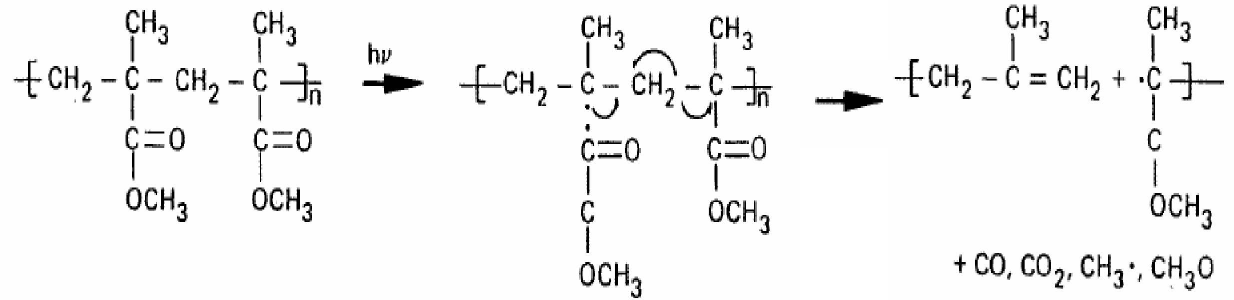

Figure 2.8 Radiation-induced main-chain scission of PMMA [10]

Although mostly referred to as a e-beam resist, PMMA has also been considered to be used in DUV lithography. DUV exposure presents an interesting situation as it is the transition between photochemistry and radiation chemistry, where photon energy coincides with material absorption bands but also with energy in excess of C-C bonding energy. The Norrish Type I reaction shown in Figure 2.8 can be activated by DUV exposure with very high dose. It is reported that the dose for PMMA is around 1-1.5 J/cm^2, which is nearly ten times higher than Chemically-amplified resist [11]. This lack of sensitivity and its corresponding impact on production throughput is a big challenge for developing PMMA derivatives as a mature DUV resist system. Besides, PMMA is a less efficient plasma or reactive ion etch mask than resists based on aromatic materials such as Novolak/ DNQ. Figure 2.9 shows etch rate of several acrylate polymers including PMMA normalized to NPR-820 [12]. The etch rate of PMMA is twice faster than Novolak resist NPR-820:

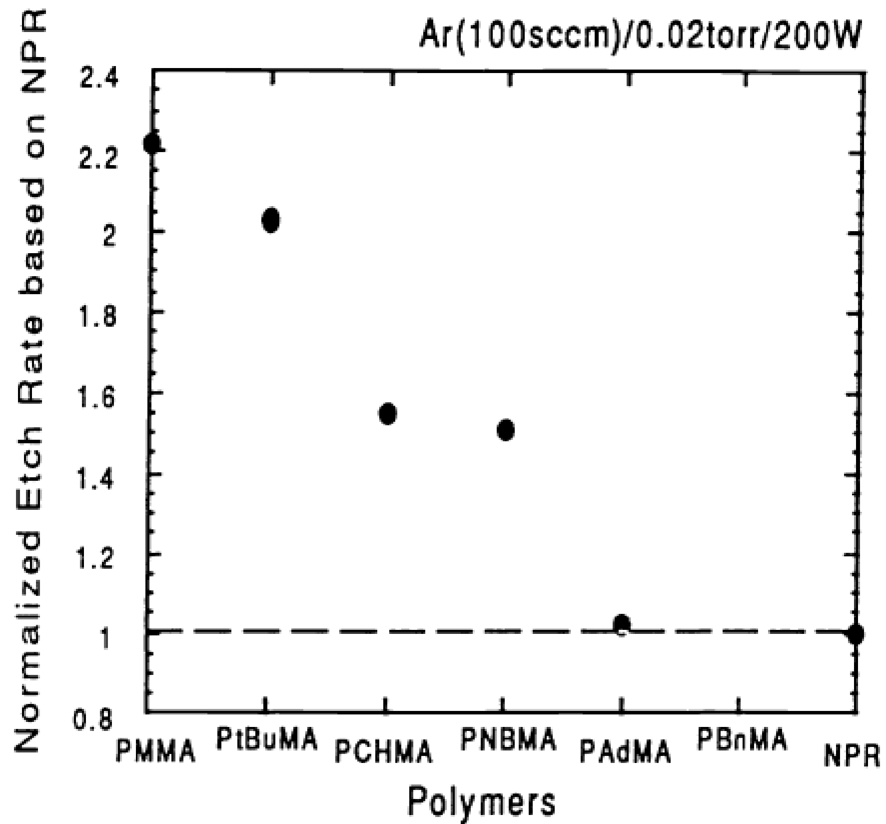

Figure 2.9 Normalized etch rate of acrylate polymers in Ar etching normalized to NPR-820 [12]

2.2 Limitations of Chemical Amplified Photoresist

Chemically-amplified resist has been widely used as commercial DUV resist for years. It consists of photo-acid generator (PAG) and polymer protected by acid-labile group. The catalytic action of the photo-generated acid on the photoresist polymer during a post-exposure bake (PEB) step causes a change in the dissolution rate in the exposed areas of the film. A single photo-generated catalyst molecule can facilitate hundreds of chemical reactions that alter the solubility of the exposed regions and thereby provide chemical amplification of the exposure dose. As the requirement of IC device fabrication goes into sub-32nm regime, the application of CA resist in 193nm lithography is

challenged. Although PMMA (via high-energy-radiation induced chain-scission) has achieved resolution to 20 nm, CA resists had not come close to this resolution [13]. The very different imaging mechanism involving thermally driven acid-catalyzed processes is summarized in Figure 2.10 [13]. These limiting factors include the following:

1. Acid gradients at exposed/unexposed interface

2. Trace amount of background acid in "unexposed" regions becomes much larger at lower k factors

3. Acid diffusion during post-exposed bake

4. Swelling and statistical dissolution effects at line edge

5. Small number of high-energy photons in small areas of high-sensitivity resists (shot noise)

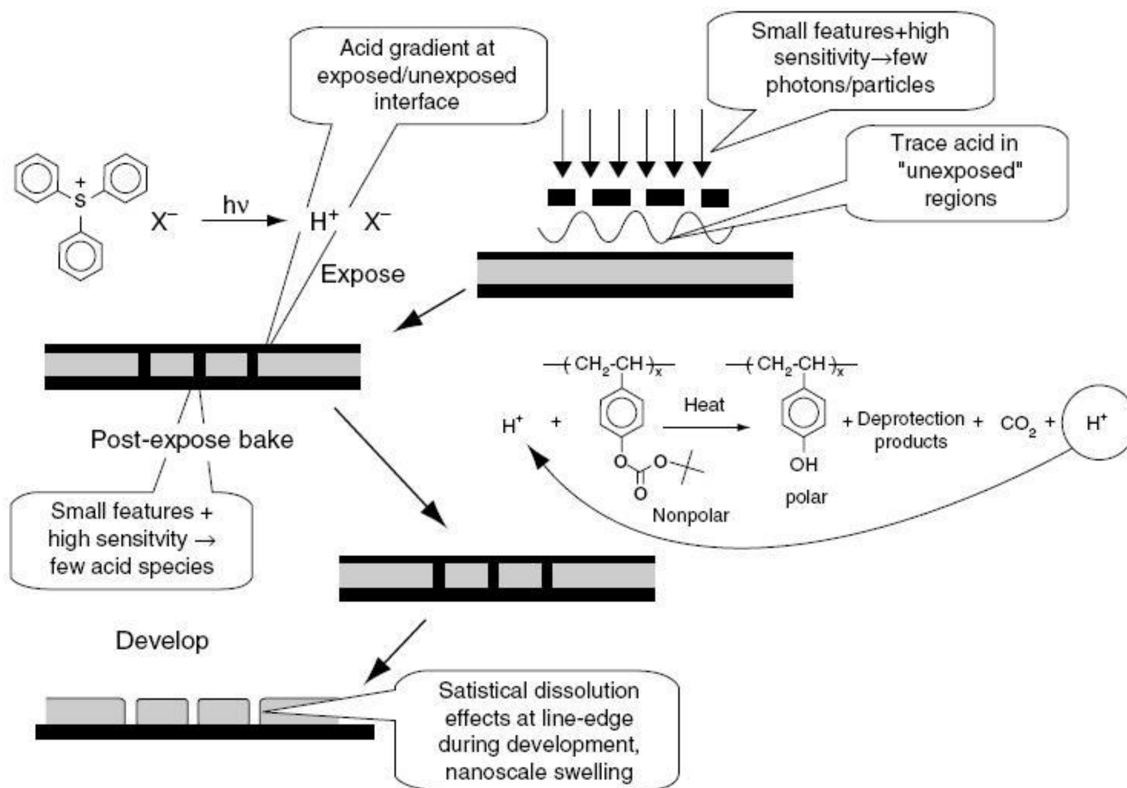

Figure 2.10 Origin of limiting factors in chemically amplified resists [13]

Among these limitations, acid diffusion is the most important one to prevent the application of Chemically-amplified resist to be used in sub-32nm lithography. In order to activate the de-protection process, the resist needs to be baked at elevated temperature after exposure (PEB). The acids generated in this reaction keep wandering around to react with other polymer molecules. The high temperature enhances the acid diffusion length and therefore, some of the acids in exposed area diffuse into unexposed area, causing Line-edge roughness. This process is shown in Figure 2.11.

Theoretical analysis predicted that the acid diffusion eventually will prevent further resolution improvement. Many researchers have been done to evaluate this

limitation of CAR. A plot of LER with focus and dose is shown in Figure 2.11, as well as the SEM imagine of 45nm dense lines using commercial 193nm CA resist [14]:

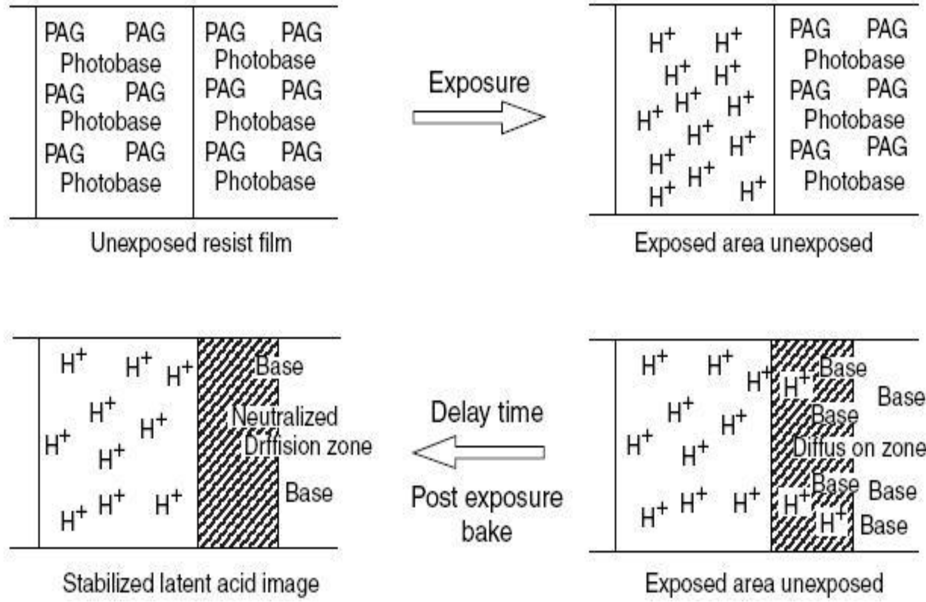

Figure 2.11 Acid diffusion in Chemically-amplified resist

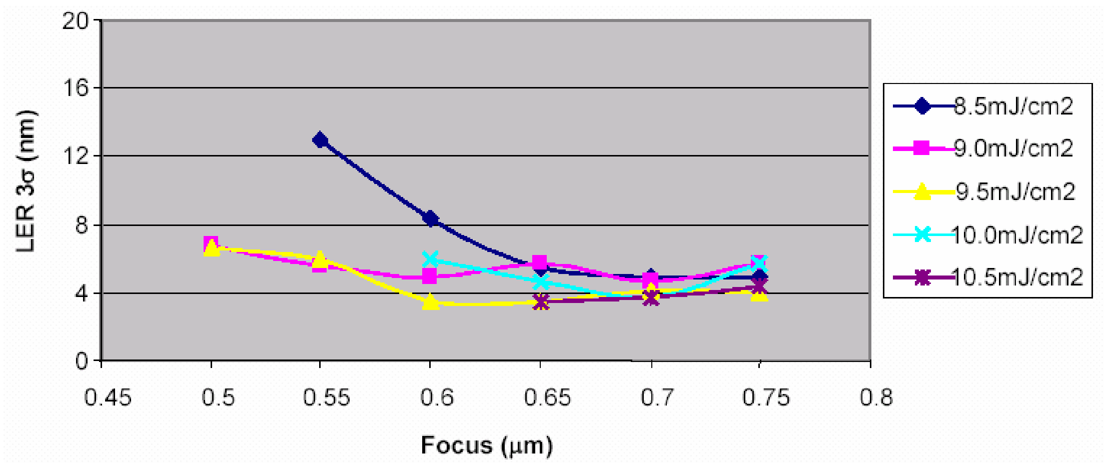

(a)

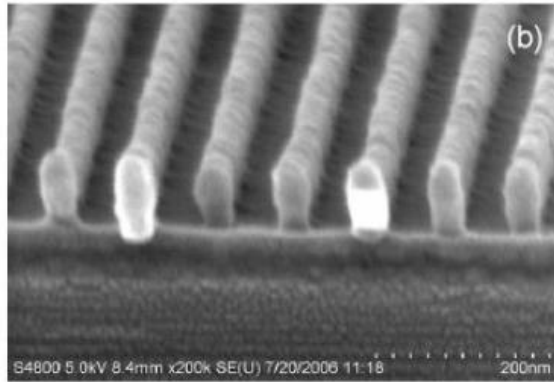

(b)

Figure 2.12 (a) LER with different focus and dose (b) top-down SEM imagine [14]

From Figure 2.12 (a), it can be seen that at best focus and dose, LER can be as low as 4nm (3σ), which is not good enough for sub-32nm feature. In the image shown in Figure 2.12 (b), both feature rounding and imagine shifting is observed, indicating poor CD control. A lot research has been going on to modify this resist system, including lower the loading of PAG, increasing base quencher concentration and using larger polymers. But all of these efforts slow down the CA resist which is inherent to chemically-amplified photoresist.

2.3 Line Edge Roughness

When variations in the width of a resist feature occur quickly over the length of the feature, this variation is called line width roughness. When examining these variations along just one edge it is called line edge roughness (LER) [15]. LER becomes important for feature sizes on the order of 100 nm or less, and can become a significant source of line width control problems for features below 50 nm. Figure 2.13 shows 1D and 2D structure of lines bearing LER problem [15]. LER is caused by a number of statistically

fluctuating effects at these small dimensions such as shot noise (photon flux variations), statistical distributions of chemical species in the resist such as photo-acid generators, the random walk nature of acid diffusion during chemical amplification, and the nonzero size of resist polymers being dissolved during development. It is unclear which process or processes dominate in their contribution to LER.

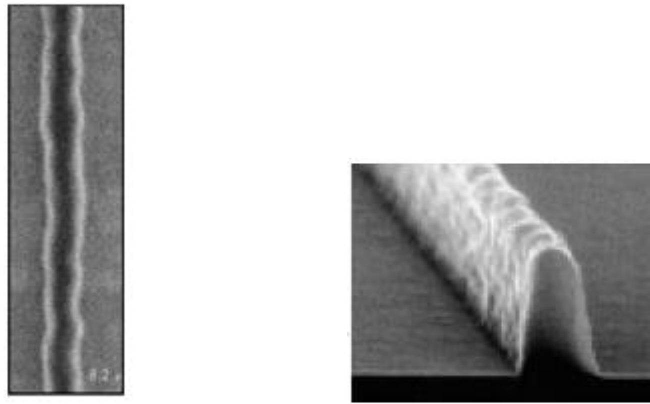

Figure 2.13 1D and 2D structure of lines showing LER [15]

LER is usually characterized as the 3σ deviation of a line edge from a straight line, though a more complete frequency analysis of the roughness can be valuable as well. For 193-nm lithography, LER values of 4 nm and larger are common. LER is inversely proportional to the normalized image log-slope (NILS), so LER generally gets worse as an image goes out of focus and for higher resolution patterns. The relationship between LER and exposure dose can be expressed by Figure 2.14 [16]. It is concluded that an increase in resolution made possible by a decrease in receptor area is accompanied by less image density and less image noise at a given level of exposure. In a word, better resolution and low LER can be achieved by sacrificing sensitivity. This is called RSL

tradeoff. This also indicates that LER problem is inherent to CA resist since it is famous of high sensitivity.

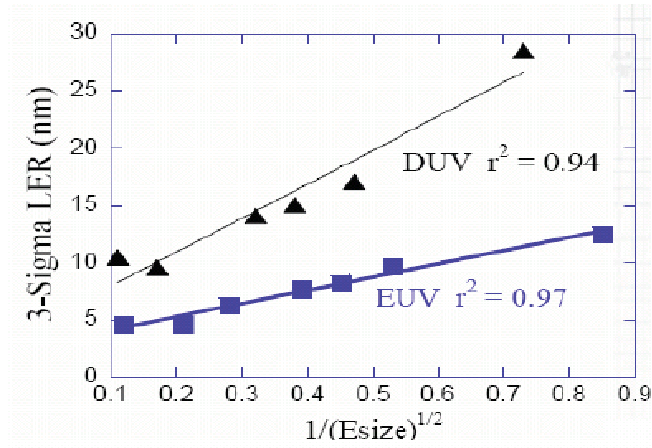

Figure 2.14 Relationship of LER and exposure dose [16]

The impact of LER on device performance depends on the specific device layer and specific aspects of the device technology. For lithography generations below 100 nm, typical specifications for the 3σ LER are about 5% of the nominal CD. It is possible that LER will become the main limit of CD control below 65-nm production.

LER is undesirable because it increases off-current (I_{off}) and causes a random variation of device currents across a die. As device size shrink, the sensitivity of LER increases. Figure 2.15 shows measurements of saturation drain current (I_{Dsat}) distribution with LER (3σ) for 70nm and 34nm device [16]. It was found that 3σ LER need to be limited to 3nm for 34nm device in order to keep performance degradation and current distribution to the same percent as the 70nm device. According to ITRS roadmap, to meet the requirement of IC devices, LER need to fall below 2nm 3σ by 2013 and below 1nm by 2019 [4]. Since the best LER would be 4nm for chemically-amplified resist as

mentioned in previous section, 50% reduction needs to be achieved for further development in photo lithography. Current photoresist system may not meet this requirement.

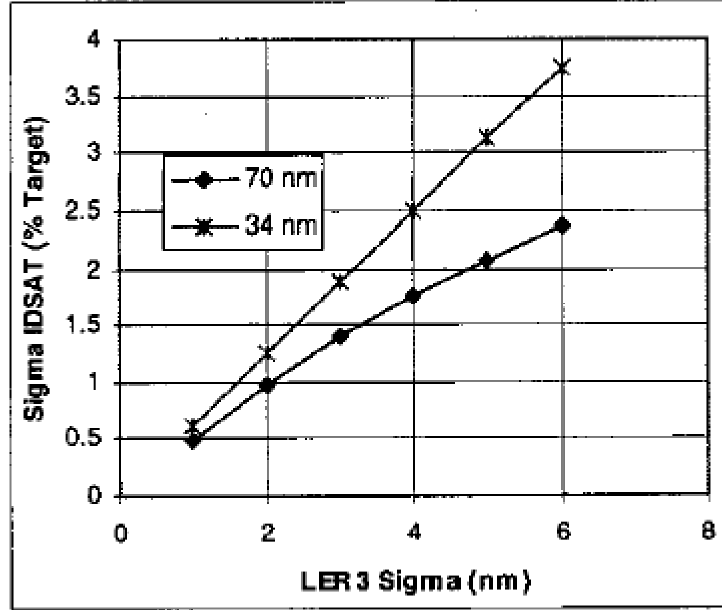

Figure 2.15 saturation drain current (I_{Dsat}) distribution with LER (3σ) for 70nm and 34nm device [16]

2.4 Optical Materials for 193nm Optics

The bulk of the optical material used for 193nm optics is fused silica, with low absorption (T internal ≥88%/cm@185nm) and thermal dispersion (dn/dT=20.6 ppm/K @193.00nm) [17]. In addition to absorption and scatter, minimizing any radiation-induced changes in optical properties is always critical to ensure a long practical lifetime of projection optics. Early concern over laser induced damage of fused silica uncovered compaction and color center formation as primary failure modes. Compaction results in a

decrease in the optical path, causing wavefront aberrations in the lens. Excimer laser induced compaction has been identified as a two-photon process. At low levels, compaction is known to increase linearly with the number of pulses and as the square of the peak intensity within a laser pulse [18]. In a 5-20 ns excimer pulse, high peak intensities are generated by relatively low values of beam intensity. Early estimates were made for a 10-year lifetime of a 193-nm fused silica lithographic lens for an energy density below 1 mJ/cm^2 per pulse within any element of the lens [19]. This restriction led to the clear need of chemically-amplified photoresist with dose requirement of 25 mJ/cm^2 based on a 50 wph throughput of 150 mm wafers. It was understood at the time that higher-dose resists could be accommodated with advances in damage resistance of fused silica and with the substitution of CaF in critical elements of the projection lens.

Crystalline calcium fluoride possesses excellent transmission characteristics at 193nm but does not have issues with compaction or rarefaction with radiation that fused silica can. Impurities such as sodium and yttrium can however result in decreased transmission [20]. Laser induced fluorescence (LIF) and transmission loss depend on the purity of the calcium fluoride. Careful attention is thus paid to these impurity levels for high quality material. Modern 193nm optics is comprised of elements of fused silica combined with calcium fluoride at critical high energy locations so that high fluency levels can be tolerated [21]. The large birefringence and inhomogeniety of calcium fluoride result in its use for only a relatively small number of elements.

The current excimer laser technology allows for ArF 193nm performance up to 6000 Hz, power to 60W, pulse energy of 10 mJ, and with >70 ns pulse length. Power to 90W is forecast in the near future [21]. By employing multipass architecture, excimer

lasers can achieve higher stability, better beam uniformity with lower peak energy density, and intrinsically longer pulse duration than earlier designs. This longer pulse duration results in a lowering of the possibility of damaging the optics within the lithography tool. Additional approaches are also used to achieve 2-4X pulse stretching, as compared to earlier designs. By combining new laser technology with the compounding of fused silica and calcium fluoride optics, a much higher energy density is permissible in 193nm projection optics. This could lead to higher throughput if irradiance at the wafer plane were the limiting determinate of throughput (which is in the 130-180 wph range now). When throughput is no longer gated by wafer plane irradiance, resist materials with lower sensitivity could be utilized.

2.5 Conclusion

As sub-32nm device generations are pursued, it becomes questionable whether current photoresist systems can meet lithography requirements. If resist sensitivity in the sub-50 mJ/cm^2 range continues to be specified, it will be difficult to achieve the resolution and feature quality (in terms of line edge roughness, LER) necessary as given in the ITRS. In 2013, for DRAM ½ pitch of 32 nm (with flash ½ pitch of 28nm and MPU gate length in resist of 21nm), resist CD control and low frequency line width roughness fall below 2nm 3σ. These values fall below 1nm by 2019. As with many photochemical systems, there is a reciprocal relationship between the sensitivity and resolution of chemically amplified resists (CAR). It is well known that increases in amplification are achieved through chemical and diffusion contributions. If both of these channels are reduced, higher resolution can be made possible. This reciprocal trade-off

may be the best route toward attaining the resolution and feature quality goals of future device generations. In this case, alternative or collaborative image pathways may need to be sought. At the mean time, development in optical materials for 193nm lithography releases the restriction of resist sensitivity. It is possible to design a new resist system by sacrificing sensitivity somehow to achieve high resolution.

Chapter 3

Design of Non-Chemically-amplified Resist

As mentioned above, the current situation in 193nm lithography requires significant change in photoresist material in perspective of both optical sources and material limitations. Non-chemically amplified resist has been expected to be the candidate of photoresist material for sub-32nm lithography. Among these non-CAR systems main-chain scissioning resist inspires a lot interest recently, especially at present when the optical sources are capable of lower through-put.

3.1 Main-chain Scissioning Resist

Classic e-beam resist PMMA achieves solubility change in organic developer by cleavage of C-C bond at the backbone through Norrish Type I reaction. Development is carried out in an organic solvent system, such as MIBK and IPA, based on the scission induced decrease in molecular weight. The free volume resulting from volatile byproducts of the scissioning reaction also contributes to development discrimination and resulting contrast. 20nm resolution has been demonstrated using this type resist in e-beam lithography. The image and structure of PMMA is shown in Figure 3.1:

(a) (b)

Figure 3.1 (a) 21.5nm lines imaged using PMMA (b) PMMA structure

Although suffering from low sensitivity, PMMA does have some advantages over chemically-amplified resist, especially in terms of LER. Figure 3.2 shows images of PMMA and CAR using e-beam lithography. The data indicates that under same condition PMMA shows smaller LER than CAR [22]. This discrimination is more obvious for smaller feature size (20nm).

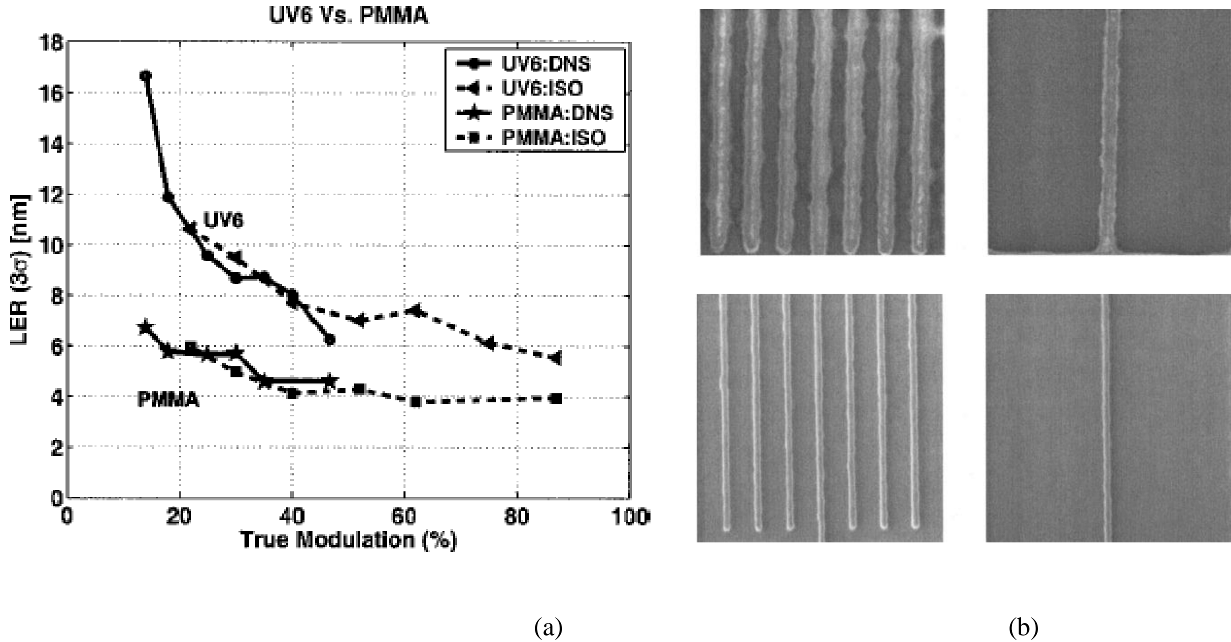

(a) (b)

Figure 3.2 (a) LER data for PMMA and UV6 for Dense and isolated lines (b) images of PMMA (down) and UV6 (up) for 100nm lines using 50 keV e-beam [22]

Since showing good performance in terms of LER, PMMA has been well investigated since long ago for its possible application in sub-32nm lithography. The influence on resist performance caused by polymer properties, such as tacticity, molecular weight was studied. Figure 3.3 shows a contrast curve for typical CAR and PMMA [23]. It can be seen that CAR contrast curve is sigmoidal in nature due to catalytic deprotection of pendant groups while PMMA exhibits linear contrast curve due direct scission of polymer chain and loss of pendant group with smaller molecules

preferentially dissolved. Generally, thickness of PMMA decreases linearly with some of the thicker film slightly offsets. Figure 3.4 shows different contrast curve for PMMA with several thicknesses [23]. It is clear that significant thin film effect observed in chain-scission mechanism in PMMA.

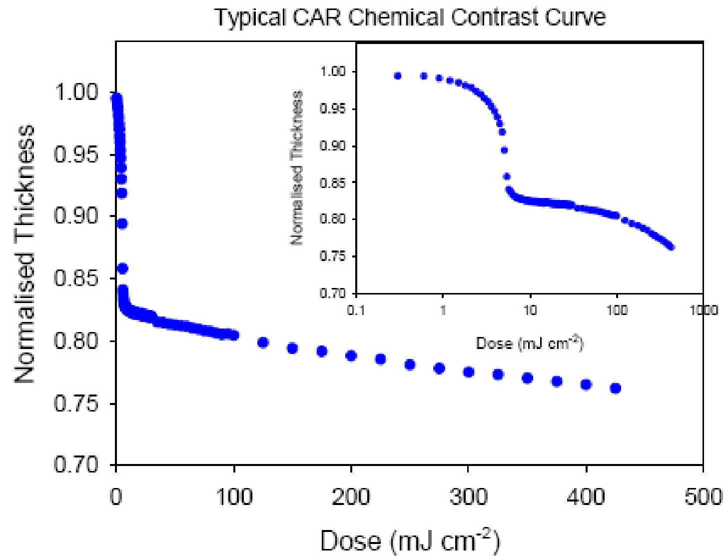

(a)

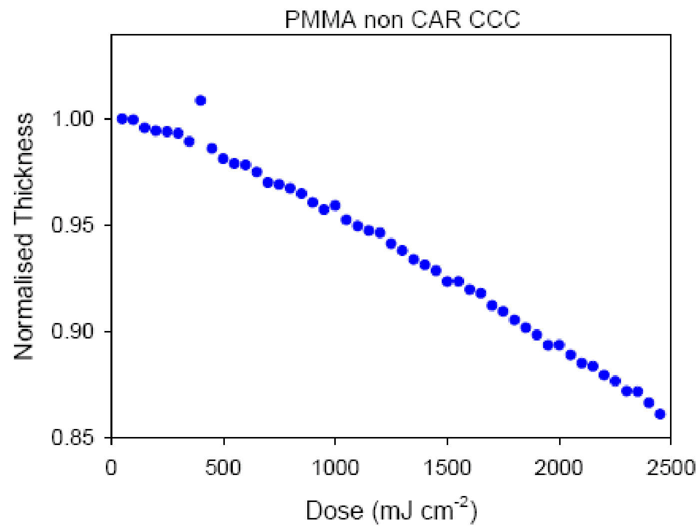

(b)

Figure3.3 Contrast curve for CAR (a) and PMMA (b) [23]

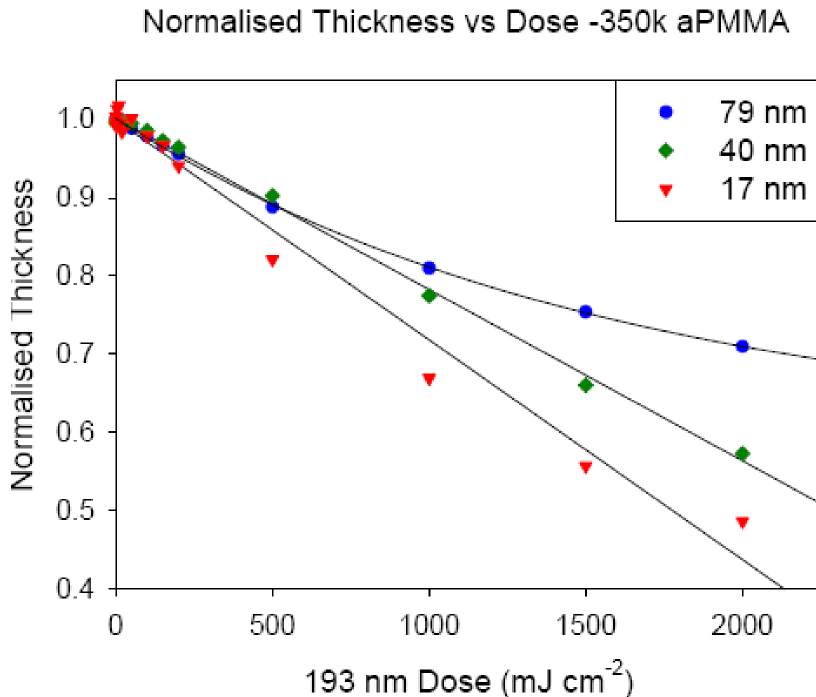

Figure3.4 Contrast curve for PMMA with thickness of 79nm, 40nm, 17nm [23]

3.2 Main-chain scissioning Resist for 193nm Lithography

As shown in figures above, PMMA show much smaller LER than CAR in 20nm features. This means it could be one of the possible candidates to replace CA resist for sub-32nm lithography considering the fact that sensitivity difference between these two kinds of resist is smaller for thin films. Some modifications are needed to improve lithographic performance of PMMA.

3.2.1 Base Solubility

The PMMA resist used in e-beam lithography is developed in organic developer such like IPA. However, most of the commercial available resists for photolithography are designed to be developed in base. Organic developer is also responsible for low contrast of PMMA. Therefore, for PMMA to be used in 193nm lithography, base

solubility need to be developed. There is already some data reported showing that some derivatives of PMMA can achieve contrast as high as ten in weak base-developer [24]. Table 3.1 shows the contrast for polymers containing different amount of Methacrylate acid (MAA):

MMA-MAA[a] Mol ratio	Molecular weight ($\times 10^{-3}$)	M_w/M_n	Developer[b]	Exposure time (min)	Contrast
4.5:5.5	322	2.8	$NaHCO_3$[c]	—[e]	—
7:3	51	2.2	$NaHCO_3$[d]	0.5	2
7.5:2.5	67	2.0	Na_2CO_3[d]	0.6	10
8:2	59	2.3	1N NaOH	—[f]	—
8.3:1.7	108	2.6	1N NaOH	—[f]	—

[a] Containing 20 w/o o-nitrobenzyl cholate.
[b] Followed by a 30 sec H_2O rinse.
[c] 5% aqueous solution.
[d] 10% aqueous solution.
[e] Entire film removed on development.
[f] No pattern is delineated upon exposure and development.

Table 3.1 Solubility and contrast of P (MMA-MAA) in weak base [24]

Significant thickness lost was observed with up to 25% acid incorporated with contrast about 10. The base developer used for this measurement has PH around 10 to 11. At the level, copolymer with 55% acids is too soluble to observe any modulation. This provides a base-developable structure that one can use to design main-chain scissioning resist for 193nm lithography.

3.2.2 Sensitivity

Reported sensitivity of PMMA is about 1-1.4 J/cm^2. The reason for the low sensitivity of PMMA can be attributed to the α-fission in the process. Improvements in the sensitivity of PMMA have been directed toward the weakening of the α C-C bond

[25]. Data has been reported that by combining other monomers in the polymer chain, sensitivity of PMMA can be increase. Some of data is shown in Table3.2 [25]:

Polymers	Exposure Dose (mJ/cm^2)	λ (nm)
Poly(methyl methacrylate) Derivatives		
PMMA	3400	240
Poly(fluorobutyl acrylate)	480	240
Poly(MMA-co-glycidyl MA)	250	240
Poly(MMA-co-3-oximino-2-butanone MA)	80	240
Poly(MMA-co-OM-co-MACN)	40	240
Polyketones		
Poly(methyl isopropenyl ketone) PMIPK	680	250
Polysulfones		
Poly(5-hexene-2-one sulfone)	500	220–400
Poly(butenesulfone)	5	189

Table3.2 Sensitivity of PMMA derivatives [25]

The improvement of sensitivity can be interpreted by formation of more stable intermediate radicals. Figure 3.5 shows photo-degradation mechanism of Poly(PIPK-MMA) [26]. It contains two pathways, one of which involves cleavage of carbonyl-carbon and main-chain carbon bond followed by electron rearrangement. The other pathway is photo-induced direct main-chain scission. Stable radical generated in both pathways favors this photoreaction. Therefore the sensitivity of this copolymer is about four times higher than that of PMMA homopolymer [26].

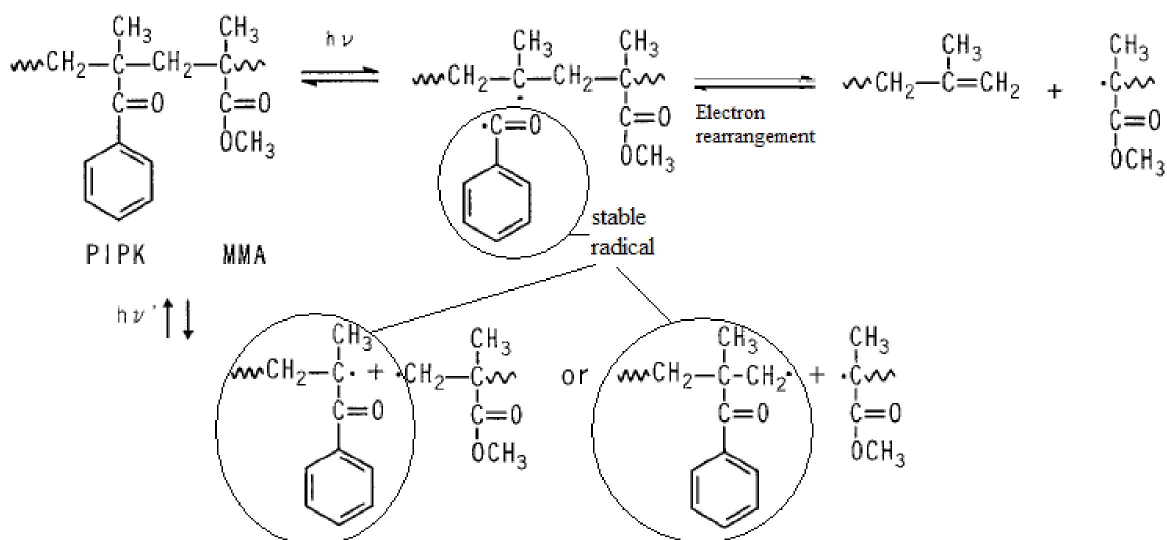

Figure 3.5 Photoreaction mechanism of Poly(PIPK-MMA) [26]

It was reported that poly(α-methylstyrene) undergo rapid chain scission upon UV radiation [27]. Photo-degradation of poly(α-methylstyrene) occurs by hydrogen abstraction from the methylene group and the formation of polymer peroxy group, as shown in Figure 3.6 (a) [27]. This polymer peroxy radical can abstract hydrogen from the same and/or neighboring polymer chain, and form polymer hydro-peroxide (Figure 3.6(b)). The polymer peroxy radical may also participate in the chain-scission reaction by the way of a six-member ring transition state (Figure 3.6(c)) [27].

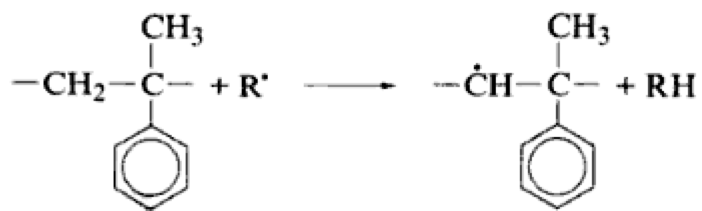

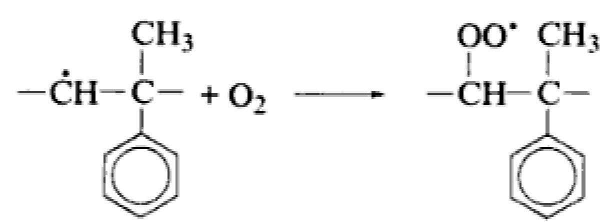

(a)

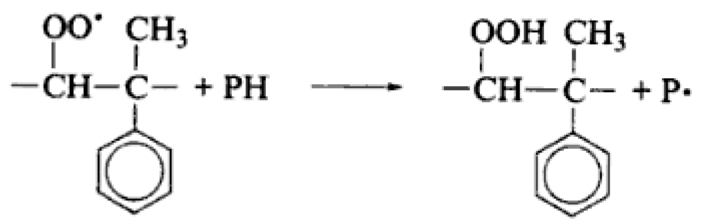

(b)

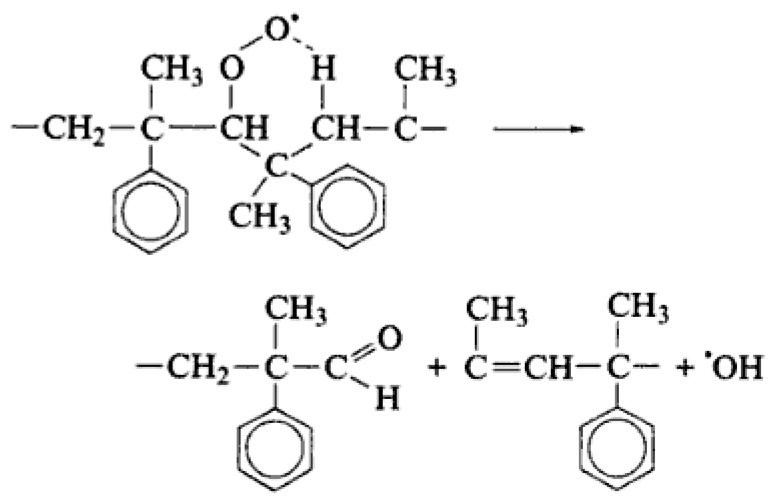

(c)

Figure 3.6 (a) Formation of polymer peroxy radical (b) Chain-scission by hydrogen abstraction (c) Chain-scission through six-member ring transition state [27]

The rapid photo-degradation of poly(α-methylstyrene) is due to formation of stabilized intermediate radical by aromatic and methyl group. Incorporating this monomer in PMMA main chain will result in enhanced chain-scissioning efficiency caused by mechanisms induced by α-methylstyrene shown in the figures above.

Some other polymers which contain tertiary-carbon side-group can improve chain-scission mechanism by going-through additional side-chain scissioning. The photo degradation process of t-butyl methacrylate is shown in Figure 3.7. As well as the main-chain scissioning induced by Norrish type I reaction and rearrangement (pathway 2 in Figure 3.7), it can also go through β-scission process at tertiary carbon-oxygen bond, forming stable methyl radical (pathway 1 in Figure 3.7). By introducing t-butyl methacrylate (TBMA) in to the polymer backbone, sensitivity can be improved because methyl radical formed in pathway 1 is very stable and this side-group scissioning is favored.

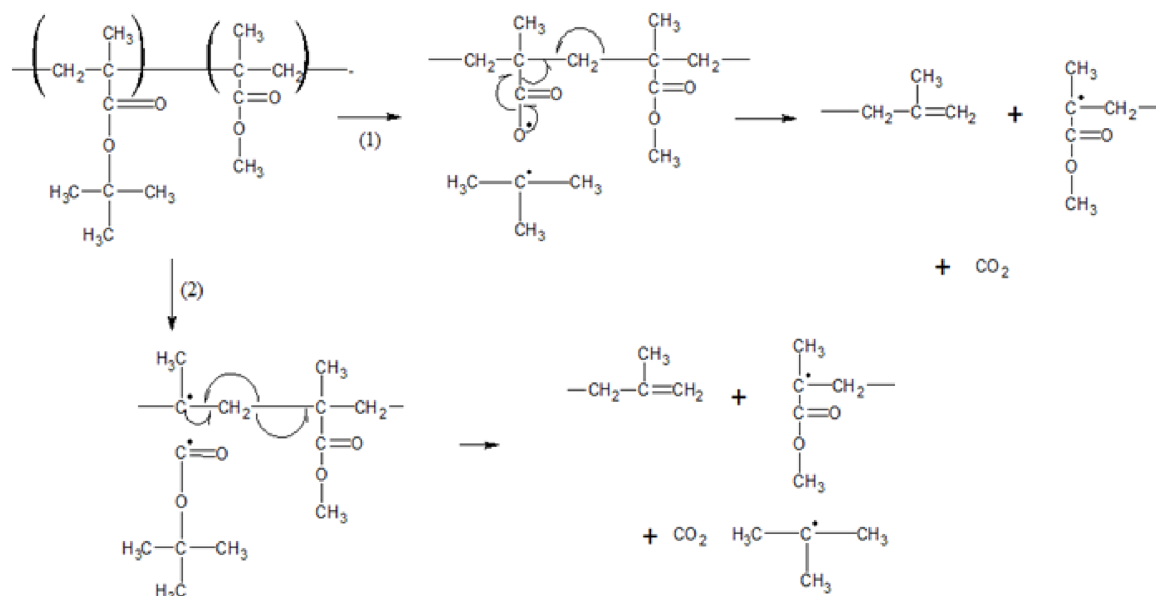

Figure 3.7 Photoreaction of TBMA

3.2.4 Etch Resistance

The center function of a patterned resist image is to provide a protective mask for the underlying substrate in the covered area. Although it seems clear that acrylic-based polymers are well suited for high resolution imaging applications at exposure wavelengths down to 193 nm, the chemical durability of this class of polymers is, in general, too low to withstand the harsh plasma etch steps required to transfer the resist pattern into underlying substrates. Etch resistance is one of the primary design considerations for polymers synthesized for 193nm photoresist because novolak-based photoresist, which happen to have high chemical stability and resistance to chemical attack, is not usable for its high absorbance.

The aforementioned polymer, containing MMA, MAA, αMEST and TBMA, has very poor etch resistance. Additional monomer needs to be incorporated into the polymer backbone to provide etch resistance. Adamantyl methacrylate is traditionally used in acrylate-based polymers to provide etch resistance [9]. This monomer is also chosen to give plasma etch resistance. However, adamantyl group tends to crosslink upon exposure. This mechanism competes with chain-scissioning mechanism so that the sensitivity decreases. The composition of this polymer needs to be carefully designed so that it has relative high sensitivity and etch resistance. Based on these considerations, the targeting polymer structure is sketched in Figure 3.8:

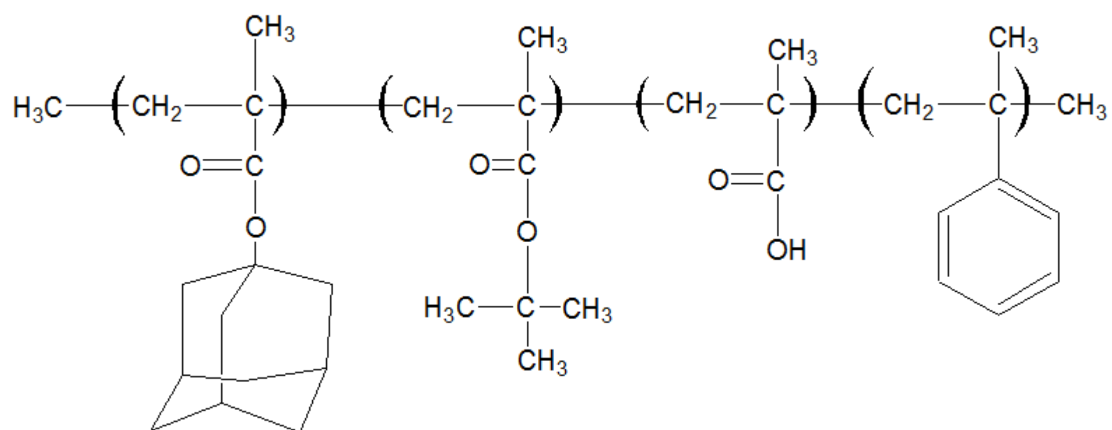

Figure 3.8 Targeting copolymer Poly (ADMA-TBMA-MAA-αMEST)

Chapter 4

Experimental Approach

As described in previous sections, it is possible to develop a main-chaining scissioning resist system that can be used in 193nm optical lithography which can be base-developed and has relatively high sensitivity. Based on the targeting polymer structure stretched in Figure 3.8, copolymers with different component have been synthesized and compared to demonstrate the theory described in previous sections.

4.1 Material Synthesis

The monomers used in synthesizing copolymers were purchased from Sigma-Aldrich, USA expect 1-Adamantyl methacrylate (ADMA), which was purchased from Bimax Chemicals Ltd, USA. The initiator used in all polymerization was AIBN, which was recrystalized from methanol at -30 ℃.

4.1.1 PMMA and P(MMA-co-αMEST): PMMA homopolymer and copolymers with different amount of αMEST (1 wt%, 2 wt% and 3 wt%) were prepared by free-radical polymerization. Monomers and initiator (0.1 wt% or 0.5 wt% to monomers) were mixed in a 500mL flask (or polymerization tubes) and purged with argon for about 20 mins. The monomer mixtures were then sealed and immersed into an oil bath held at 68 ℃ for overnight. Ethyl acetate was used as solvent and IPA was used as the chain transfer agent in all the polymerizations involving αMEST.

4.1.2 P(MMA-co-MAA): Two copolymer sets were prepared. One was a control composition with 25 mol% MAA and 75 mol% MMA. Another contained 25 mol%

MAA, 68 mol% MMA and 7 mol% αMEST. For both copolymer sets, 10 g of monomers were charged into a sealed tube with 20mL of solvent, ethyl acetate, and 0.1 wt% of AIBN. The mixture was purged with Argon for 20 mins and immersed overnight into an oil bath held at 65 ℃.

4.1.3 P(MMA-co-TBMA-co-MAA): TBMA was incorporated the copolymer composition because it has been reported to enhance chain-scissioning efficiency. Ten grams of monomers (15 mol% MAA, 39 mol% TBMA, 39 mol% MMA and 7 mol% αMEST) in total were charged to a sealed tube with 20mL ethyl acetate And 0.1 wt% (based on monomer) of AIBN. The mixture was purged with argon for 20mins and immersed in an oil bath held at 65 ℃ for overnight.

4.1.4 P(ADMA-co-TBMA-co-MAA): ADMA was incorporated in the polymer system to provide etch resistance. Two copolymer sets were designed and synthesized. One was P(ADMA-co-TBMA-co-MAA-co-αMEST) with a molar ratio 39:39:15:7. Another was P(ADMA-co-MMA-co-TBMA-co-MAA-co- αMEST) with a molar ratio 20:19:39:15:7. Eight grams of monomers in total were charged to a sealed tube with 16mL of ethyl acetate and 0.05 wt% of AIBN (base on monomer). The mixture was purged with argon for 20 minutes and immersed overnight in an oil bath held at 65 ℃.

4.1.5 Polymer Isolation: After cooling to ambient temperature, all the copolymer solutions were precipitated in hexanes, centrifuged and decanted. Isolated wet solid polymers were air-dried overnight.

4.1.6 Molecular Weight and Composition: Styrene-equivalent molecular weights were obtained by standard gel permeation chromatography, eluting with

tetrahydrofuran (THF) over an Agilent trimodal S column set with a 0.5-1000K molecular weight range. Copolymer composition was evaluated by NMR.

4.1.7 Polymer Film Fabrication and Characterization: The solid polymers were dissolved in Cyclopentanone at 1%, 3% or 10% by weight depending on the molecular weight, forming photoresist. The copolymer solution was then spin-coated on 6' wafer with desired thicknesses. Silicon wafers were dehydration baked for 2 mins at 200˚C. HMDS and BARC were selectively used depending on adhesion and optical characteristics desired. Prebake temperature was 140°C (or 145°C) for 1 min. Optical parameters of polymer films were determined by ellipsometry (WVASE) and the film thicknesses were measured on a Prometrix SpectraMap FT500. In order to measure the absorbance of resist materials coated on a fused silica, a Perkin-Elmer Lambda 11 UV-Vis spectrophotometer was used.

Exposures were carried out by using open frame at 193nm using an ArF excimer laser by covering a broad range of doses. The developers chosen were weak base, such like sodium bicarbonate, sodium hydroxide and diluted TMAH (0.26N, CD-26). Development time was usually set to be 1 min. Etch resistance of copolymers are measured using Drytek Quad in cleanroom. The Amphibian XIS is used to expose coated wafers to print dense features at different pitch values. The quality of imaging is evaluated by SEM imaging.

Chapter 5

Result and Discussion

5.1 Enhancement of Sensitivity

In order to increase chain-scission quantum yield, certain absorptive monomers can be incorporated in the main-chain of a copolymer to induce scission at the point as which energy is absorbed. If absorption is too large, problems such as image scum can occur. α-Methyl Styrene (αMEST) is such a strong absorptive monomer which, when incorporated in the polymer chain, tends to enhanced chain cleavage. A PMMA homopolymer control and copolymers with 1% and 3 wt% of αMEST were synthesized. UV spectra are shown in Figure 5.1. By incorporating αMEST into PMMA copolymers, the absorption in DUV region is dramatically increased even with 1 wt% of αMEST.

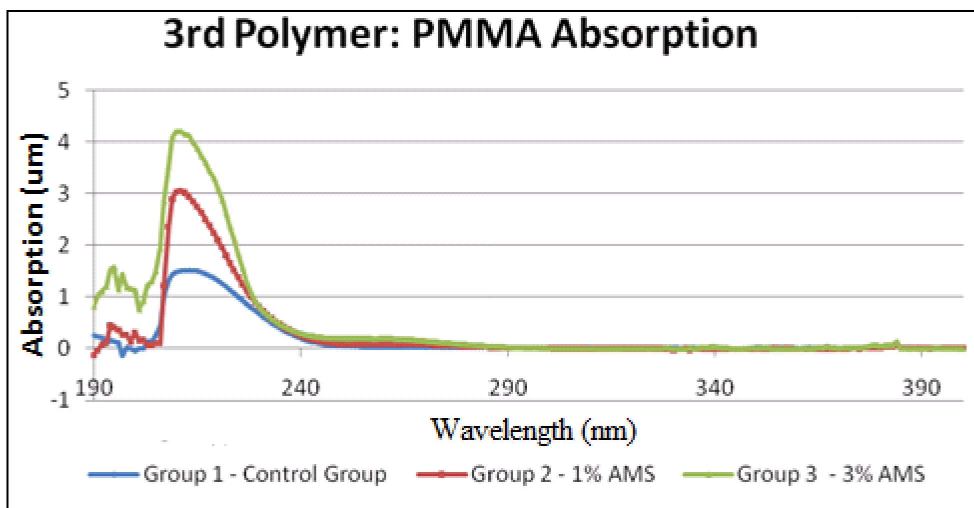

Figure 5.1

UV-spectral result for PMMA derivatives.

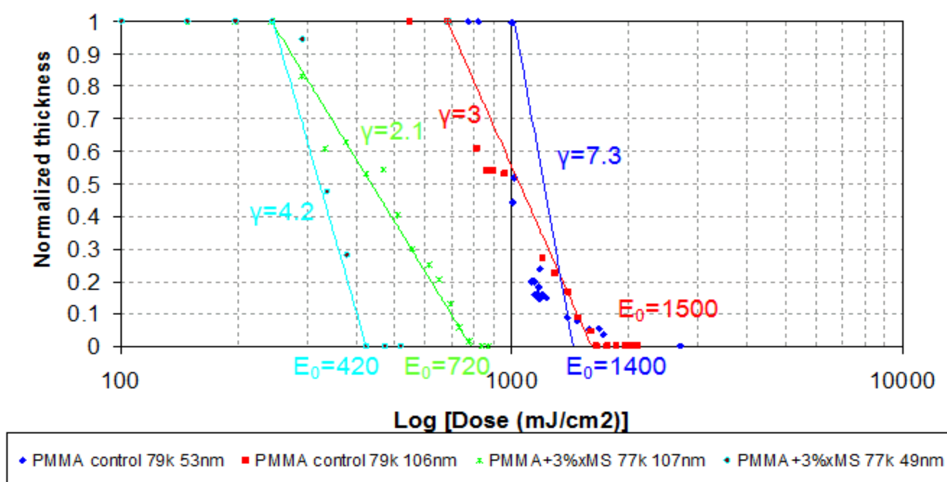

Figure 5.2 Contrast curve in organic developer for PMMA with comparable molecular weight for different film thickness

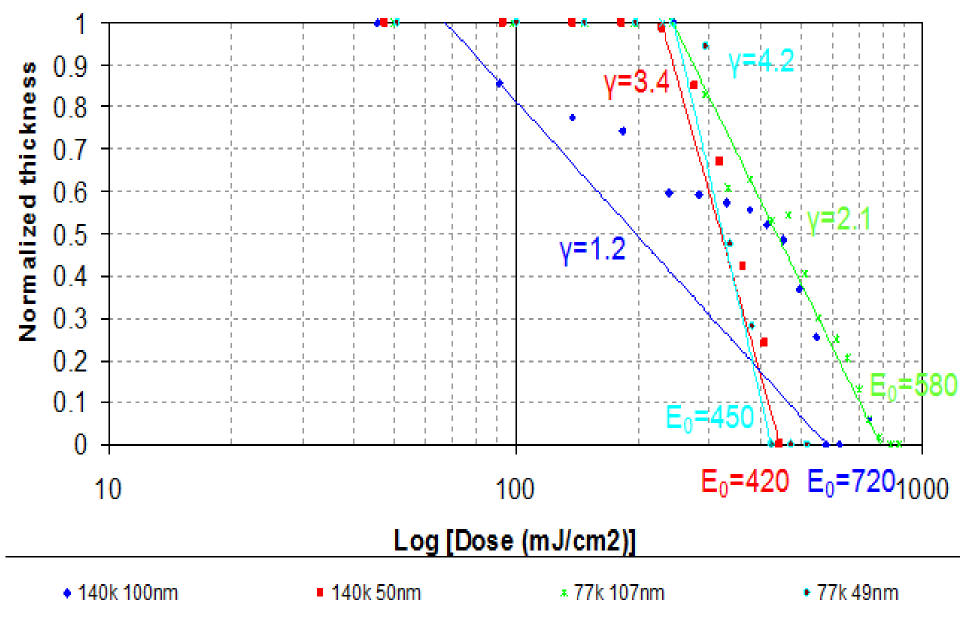

Figure 5.3 Contrast curve in organic developer for P(MMA-co- αMEST) for different molecular weight and film thickness

Figure 5.2 and 5.3 are contrast curves for PMMA control group and copolymers of MMA with different amount of αMEST. From Figure 5.2, it can be seen that the dose-to-clear value of PMMA homopolymer for 107nm film is around 1500mJ/cm^2. This

number matches the data reported in literature. On the other hand, the dose-to-clear value measured for copolymer incorporating 3% αMEST is around 720mJ/cm^2. Under the same condition, 2 times increment in sensitivity has been observed for copolymer incorporating αMEST. While for 50nm film, the measure sensitivity for PMMA control group is about 1400mJ/cm^2. This value for copolymer is 420mJ/cm^2. This means for 50nm film, the copolymer incorporating αMEST shows 3 times higher sensitivity compared with PMMA homopolymer. The enhancement of sensitivity is more pronounced for thin films. This phenomenon can be explained by the stable intermediate radical generated by αMEST in photo-degradation process. The monomer αMEST also absorbs photon energy. So for thicker film, smaller difference is observed between homopolymer and copolymer.

Figure 5.3 is a set of contrast curve measure in organic developer for copolymer of MMA and αMEST with different molecular weight. Enhancement of sensitivity is observed for film thickness on the order of 100nm for larger molecular weight copolymer while nearly no enhancement can be observed for film thickness on the order of 50nm. This is because the poly-dispersity of copolymer with larger molecular weight is relatively high (over 3.0). There is a portion of small molecules in the polymer products which limits the chain-scissioning efficiency.

5.2 Base Solubility

The enhancement of sensitivity has been reported in literature and indicated by the data shown in previous section. Contrast curves shown in Figure 5.2 and Figure 5.3 were all developed in organic developer (mixture of MIBK and IPA with a ratio of 3:1). Base-solubility is also an important property for photoresist system design. Organic-

developable system is not compatible with large volume production in optical lithography and the contrast is limited as well. Figure 5.4 shows the contrast curve of P (MMA-TBMA-MAA-αMEST) (39:39:15:7). This copolymer is dissolved in Cyclopentanone to formulate a 4% photoresist solution. It was then spin-coated on a 6' wafer by the method described in previous section; forming a 45nm film. The developers used in this study are sodium bicarbonate and sodium hydroxide. They are weak base with PH value around 10-11.

In weak base, the unexposed copolymer is slightly soluble, according to this contrast curve. The solubility is higher in more polar developer, sodium hydroxide. The dose-to-clear value of this four component system is around 110mJ/cm^2. It means that this four-component polymer is more sensitive than the copolymer incorporating 3% αMEST. The further enhancement of sensitivity attributed to both t-butyl methacrylate and 7% αMEST incorporated.

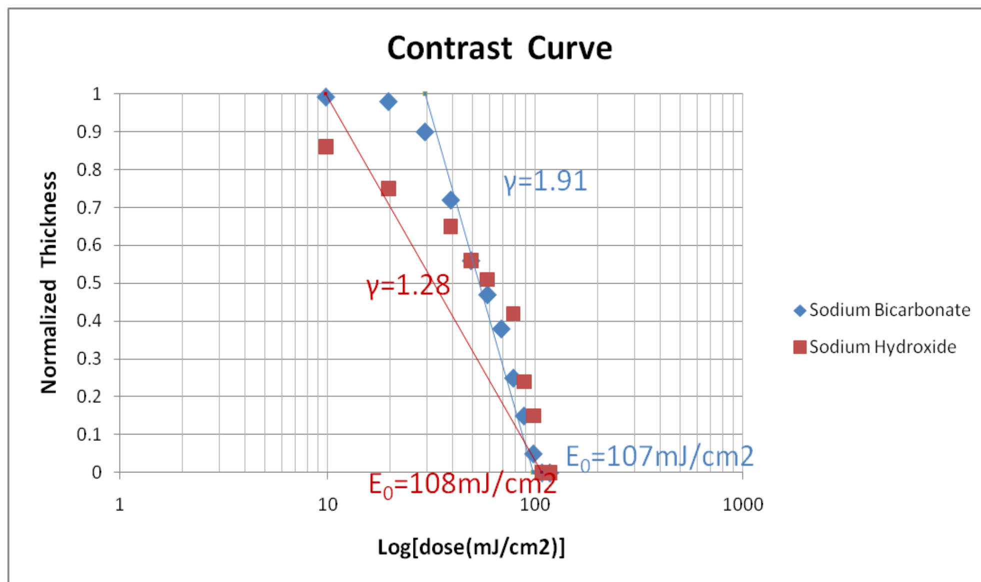

Figure 5.4 Contrast curves for polymer P (MMA-TBMA-MAA-αMEST) (39:39:15:7)

This contrast curve of P(MMA-TBMA-MAA-αMEST) proves that this four-component copolymer solution is a base-developable resist system with relatively high sensitivity and contrast (around 1.9 in sodium bicarbonate). However, the polymers tested so far have low etch resistance. Resist system without good etch resistance is not practical and can not be used as etching mask in pattern-transfer process. Therefore, additional monomer needs to be put into polymer backbone to provide this important property.

5.3 Etch resistance

As shown in Figure 3.8, polymers containing adamantyl-group were synthesized in order to improve the etch resistance. The adamantyl group provides good etch resistance because it has a carbon-ring. But it has also been reported that the adamantyl group will tend to go through cross-linking mechanism as well as chain-scissioning mechanism. Therefore, the sensitivity of the whole photoresist may be lower with presence of adamantyl-group. P(ADMA-TBMA-MAA-αMEST), whose structure is shown in Figure 3.8, was synthesized as described in Chapter 4.

Polymers were dissolved in Cyclopentanone and spin-coated on 6” wafers at a thickness of approximately 100nm. These films were irradiated at 193nm, ArF excimer laser, and exposed spots were scrapped off and rinsed into a small vial with spectra-grade THF. After about 30 minutes, the molecular weight of the polymer in the solutions was evaluated by GPC. Figure 5.4 shows the GPC results of 4 polymers. From this plot, it is clear that compared with P(MMA-MAA), the polymer incorporating 7 mol% αMEST gives much higher chain-scission efficiency. Notably, at low dose, Chain-scissioning

predominates in the copolymer containing ADMA. The molecular weight goes down with exposure dose. However, as the dose increases, cross-linking predominates and overcomes the impact of chain-scissioning in reduction of molecular weight.

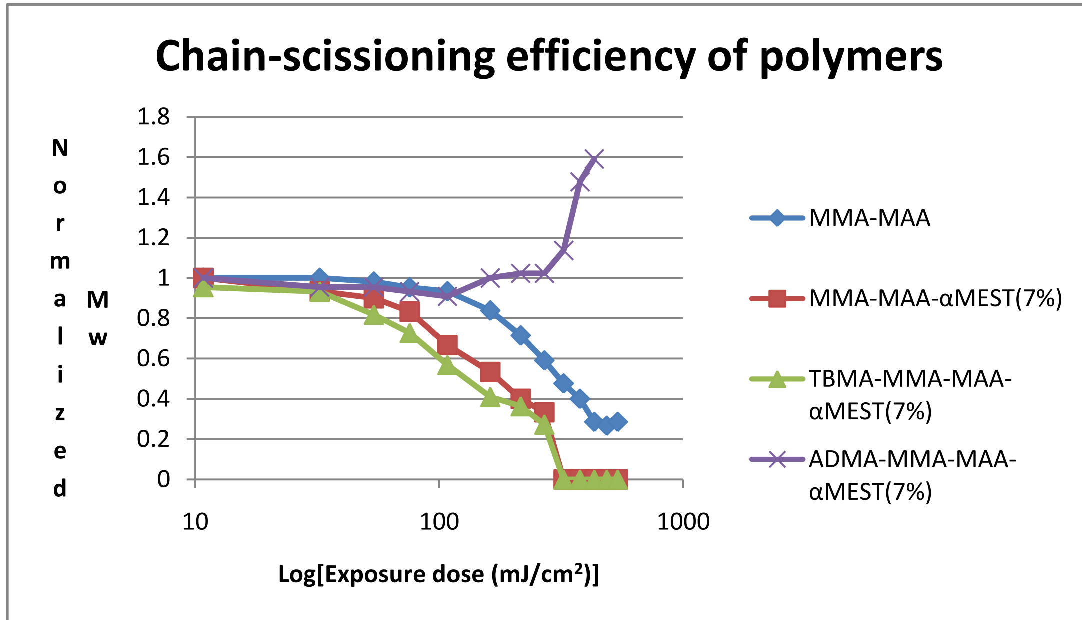

Figure 5.4 Chain-scissioning efficiency of four polymers

This set of data quantifies the cross-linking phenomenon of adamantyl-containing polymer. Although adamantyl group has been widely used to provide etch resistance in chemically-amplified resist, it is not a good choice for chain-scissioning resist, according to the plots shown in Figure 5.4. This is because the cross-linking mechanism dominates at high dose. The chemically-amplified resist, as described above, has sensitivity around 10mJ/cm^2. At this dose, deprotection mechanism is favorable. But for main-chain scissioning resist, the sensitivity could be over 100mJ/cm^2. Both chain-scissioning and cross-linking take place at this dose.

5.4 Silicon-containing Polymer

In Figure 5.4, it can be seen that the adamantyl-containing polymer goes through cross-linking instead of chain-scissioning upon exposure. This means that although P(ADMA-TBMA-MAA-αMEST) has very high etch resistance, it is not a good chain-scissioning polymer for 193nm lithography. Silicon-containing polymers have been proved to be good etch-mask in oxygen plasma etching [1]. During oxygen plasma etching of organosilicon polymers, the surface layer is converted into SiO_2 by reaction with the plasma species. The thickness of this oxide layer correlates well with the mean range of the incoming ions, roughly 10–20 nm [27], and it is formed after an initial densification phase, during which the etch rate is higher.

Methacryloxymethyl-trymethylsilane (MESI) is purchased from GELEST, Inc. Its structure is shown in Figure 5.6. 45 mol% of this monomer was incorporated to provide 10 wt% of silicon relative to the polymer. This polymer, whose structure is shown in Figure 5.7, was dissolved in cyclopentanone to make 4 wt% photoresist solutions. The sensitivity of this photoresist is around 220mJ/cm^2 for 100nm film.

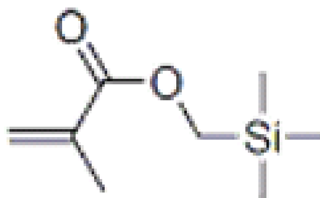

Figure 5.6 Methacryloxymethyl-trymethylsilane

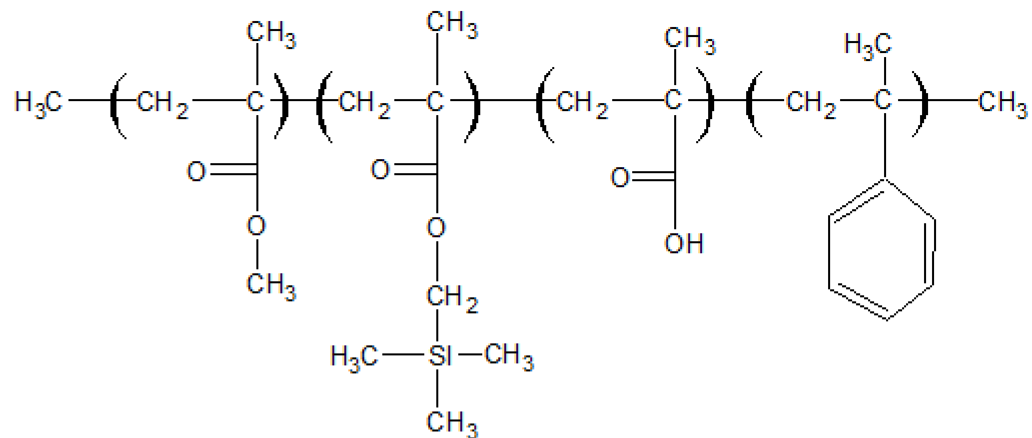

Figure 5.7 Polymer structure of P (SI-MMA-MAA-αMEST)

Oxygen plasma etch was used to test the etch rate of each polymer, as shown in Table 5.1. The etching condition is 100W for power, 25sccm Oxygen and 8mTorr for pressure. Polymer solutions were coated on 6' wafers to form around 100nm film. These wafers were etched for 5secs at first. Then upon observation, the wafers showing slight color changed were etched for another 25secs (30secs in total).

Polymer composition	Etch rate in Oxygen plasma (A/min)	Mw	Polydispersity
PMMA	NA	79k	2.72
P (MMA- αMEST3%)	NA	77k	2.73
P (MMA-MAA)	899	105k	2
P(MMA-MAA- αMEST)	765	30k	2.1
P(MMA-TBMA-MAA-αMEST)	720	44k	2.4
P(ADMA-TBMA-MAA- αMEST)	97	70k	2.4
P(ADMA-MMA-TBMA-MAA-αMEST)	NA	44k	2
P(SI-MMA-MAA-αMEST)	220	46k	2.4

Table 5.1 Parameters of polymers

The polymer contains 45mol% silicon so that the etch rate is higher than reported [1]. But it still can be seen from the data that the etch resistance for silicon-containing polymer in oxygen plasma is much better than any other polymers tested. As expected, the adamantyl-containing polymer gives the lowest etching rate, followed by the silicon-containing polymer. Other acrylate polymers show very high etching rate, which indicates poor etch resistance.

Imagines were made using four-component resist system, P(MMA-TBMA-MAA-MEST) (39:39:15:7). They are shown in Figure 5.8. These images are 250nm hp lines. The resist film thickness is made to be 100nm and BARC was coated to be 88nm film. The film thickness is optimized by Prolith.

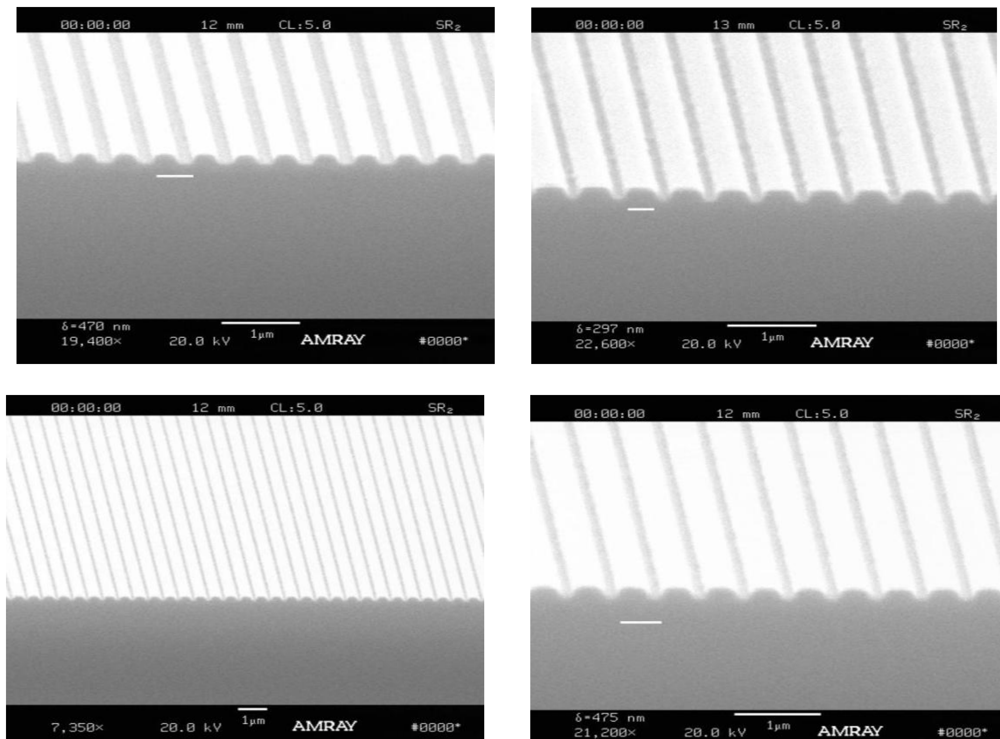

Figure 5.8 250nm features of P(MMA-TBMA-MAA-αMEST) (39:39:15:7)

The image quality is good. Very small line-edge roughness can be seen from these pictures. However, the feature size is 250nm. It is too large to exam the LER problem which is on the order of 3 to 4nm. This project is targeting 100nm feature size or below. But the process widow in base developer is found to be very narrow. Therefore it is difficult to acquire smaller images based on current resist design.

Chapter 6

Conclusion

In this project, the potential application of main-chain scissioning resist in 193nm lithography is explored. The acrylate-based polymers (mainly PMMA) have been used traditionally as main-chain scissioning resist for e-beam lithography. This kind of resist has certain drawbacks which prevent it from being used in 193nm lithography, including low sensitivity; poor etch resistance and low contrast. The designed photoresist in this project based on main-chain scissioning mechanism is base developable and has relatively high sensitivity and etch resistance. Several progresses have been made in this project:

(1) Base-developable photoresist based on main-chain scissioning mechanism were formulated. It has been proved to have relatively high sensitivity and contrast.

(2) T-butyl group can improve the sensitivity by providing side-chain scissioning.

(3) Adamantyl-incorporated polymer has good etch resistance. However, the data measured by GPC shows that it tends to cross link upon exposure other than chain scission.

(4) Silicon-containing polymers provide good etch resistance in oxygen-plasma etch.

In this project, a resist system, which is based on main-chain scissioning mechanism, is developed for 193nm lithography. It has relatively high sensitivity and good resolution for 240hp features. However, this resist system is not a good etch mask. Although this problem is solved by incorporating silicon into the polymer backbone of

the polymer film. More future work needs to be done on the silicon-containing chain-scission photoresist for 193nm lithography. Because the developer used in this project is diluted CD26, the process window turns out to be very small. It is very hard to make smaller features out of this resist system, which means it is still not a mature system. However, it is proved in this project that non CAR system is possible to be designed for 193nm lithography.

Reference

[1] J. R. Sheats and B. W. Smith "*Microlithography: Science and Technology*" 2nd Edition 2007

[2] "International Technology Roadmap for Semiconductors 2006 update, Lithography." *vol. 2006, 2006*

[3] G. Moore. 1965. "Cramming more components onto integrated circuits" *Electronics, 38:8, 114–117.*

[4] ITRS. (2009, International Technology Roadmap for Semiconductors 2007 Edition Lithography. Available: http://www.itrs.net/reports.html

[5] G. E. Moore, "Cramming more components onto integrated circuit" *Proceedings of the IEEE. vol. 86 [New York, N.Y.]: Institute of Electrical and Electronics Engineers, 1998, p. 82.*

[6] L. Burn Jeng, *J. Vac. Sci Tech, vol. 12, pp. 1317-1320, 1975.*

[7] Hanabata, M., Uetani, Y., and Furuta, A., *J. Vac. Sci. Technol. B, vol. 7, pp 640, 1989*

[8] H. Ito and C.G. Willson. *1983. ACS Symposium Series, vol. 242*

[9] Allen R. D., Wallraff G. M., Hinsberg W. D., Simpson L. L., *J. Vac. Sci Tech. B, Vol. 9, pp. 3357-3361, 1991*

[10] Larry F.Thompson, C.Grant Willson, "Introduction to Microlithography" 2nd Edition

[11] Dan E., Guillet J.E., *Macromolecules, Vol. 4, 375, 1971*

[12] Yuko K., Koji N., Satoshi T., Naomichi A., *Proc. SPIE, Vol. 1672, 66, 1992*

[13] Hinsberg W., Houle F., Sanchez M., Hoffnagle J., Wallraff G., Medeiros D., Gallatin G., Cobb J., *Proceedings of SPIE*, 5039, 2003

[14] Yayi W., Markus B., Wolf-Dieter D., Antje L., Michael S., *Proc. of SPIE Vol. 6519, 2007*

[15] Mack C.A., Field Guide to Optical Lithography, *SPIE Press, Bellingham, WA (2006)*

[16] Linton T., Chandhok M., Rice B. J., Schrom G., *IEDM Technical Digest*, *2002*

[17] Rothschild M., Sedlacek J. H. C., *Proceedings of SPIE*, *Vol. 1848, 537, 1992*

[18] Kittelman O., Ringling J., *Opt. Lett. vol. 19, 2053, 1994*

[19] Rothschild M., Sedlacek J. H. C., *Proceedings of SPIE*, *vol. 1848, 537, 1992*

[20] Kittelman O., Ringling J., *Opt. Lett. vol. 19, 2053, 1994*

[21] Brown D.J.W., O’Keeffe P., Fleurov V.B., *Proceedings of SPIE*, *Vol. 6520, 537, 2007*

[22] Ma T., Cerrina H., *J. Vac. Sci. Technol. B,Vol. 21, No. 6, 2003*

[23] Idriss B., Lan C., Yong-Keng G., Andrew K. W., *The University of Queensland, Australia*

[24] Reichmanis E., C. W. Wilkins, Chandross E. A., *J. Electrochem. Soc., vol. 129, Issue 11, pp. 2552-2555 1982*

[25] A. Reiser, Photoresctive Polymers, the Science and Technology of Resists, *Wiley Interscience, p 277, 321, 1989*

[26] Kazuyuki S., Toshiko H., Masahito K., Kieko H., Kyoichi S., *Polym. J., vol. 35, No. 12, 2003*

[27] Jan F. Rabek "Polymer photodegradation: mechanisms and experimental methods" Page 210, 1995

[28] Hartney M. A., 1988. PhD thesis, Department of Chemical Engineering, University of California-Berkeley.